Dear reviewer,

We all really appreciate your careful reading and hard work on this manuscript. These constructive opinions help to improve our work to a great extent. We did our best to respond to each comment and make this work well-organized. With the help of your detailed comments, some mistakes in the original manuscript were found and revised.

This paper presents an analysis of the relationship between turbulence statistics and $PM_{2.5}$ concentrations. The authors identify a typical pattern of haze pollution and attribute this pattern to the evolution of turbulent eddies. However, the paper lacks theoretical rigor and contains basic errors. The primary issue of the paper is that the partitioning between sub-mesoscale motions and turbulence motions is artificial and the explanation of haze pollution pattern using this partitioning is subjective. The authors claimed the emergence of sub-mesoscales even during daytime hours, but no solid evidence is given to substantiate this claim. Accordingly, the reviewer cannot recommend publication in ACP. Below some comments are listed that may help improve the manuscript.

Response: Thanks for your constructive comments. We understand your concerns about the partitioning between sub-mesoscale motions and turbulence motions. We are sorry for not elucidating it clearly in the original manuscript. We realize the insufficient introductions and descriptions in the original manuscript make this part of contents confused to readers. Thus, we intended to make substantial corrections to the original manuscript. And we would like to reply this from the following mainly three aspects:

(1) The concepts we follow. Our current study follows the literature and perspectives in the field of atmospheric turbulence in the atmospheric boundary layer, including the definition of sub-mesoscale motion by Mahrt et al., the basis for partitioning between sub-mesoscale motions and turbulent motions, and the classical turbulence energy spectrum model.

(2) The existing sub-mesoscale motions results in literatures. We will introduce the existing studies on the definition of the spectral gap between sub-mesoscale motions and turbulent motions and the emergence of sub-mesoscale motions during the daytime hours, including the original descriptions and figures in literatures.

(3) The direct observational time series in our study. The sub-mesoscale motions in the urban canopy layer (UCL) are introduced in detail through the actual observed cases in this study, which will be presented from the perspective of turbulence fluctuation. In addition, we also explain that the existence of rough elements in the UCL causes turbulence to appear non-stationary and non-uniform, and turbulent motions are strongly affected by the sub-mesoscale motions.

The details are presented in each response below.

1. The paper is motivated by the unique features of urban boundary layer in basins. So, how the observed haze pollution pattern differs from non-urban areas?

Response: Thank you for your insightful comments. The haze pollution pattern observed in the UCL of this basin city indeed differs from non-urban areas in previous studies, and it is also different from other cities which are not in a basin, such as Beijing and Tianjin in the North China Plain.

Our observation platform was located in the UCL of Lanzhou Basin, China, and this study has identified a typical evolution pattern of haze pollution within the UCL: $PM_{2.5}$ concentrations rose from 08:00-13:00, declined from 14:00-18:00, rose again from 19:00-21:00, and decreased from 22:00-07:00. As illustrated in Figure 1e and Figure 2a, haze pollution pattern observed in non-urban areas did not exhibit obvious characteristics. These results are cited from Li et al. (2020) and Jia et al. (2022), in which the observation sites were located in non-urban areas, specifically on the underlying surface of wheat fields in Baoding City, Hebei Province, China, and on the underlying surface of flat farmland in the southern suburbs of Dezhou City, Shandong Province, China, respectively.

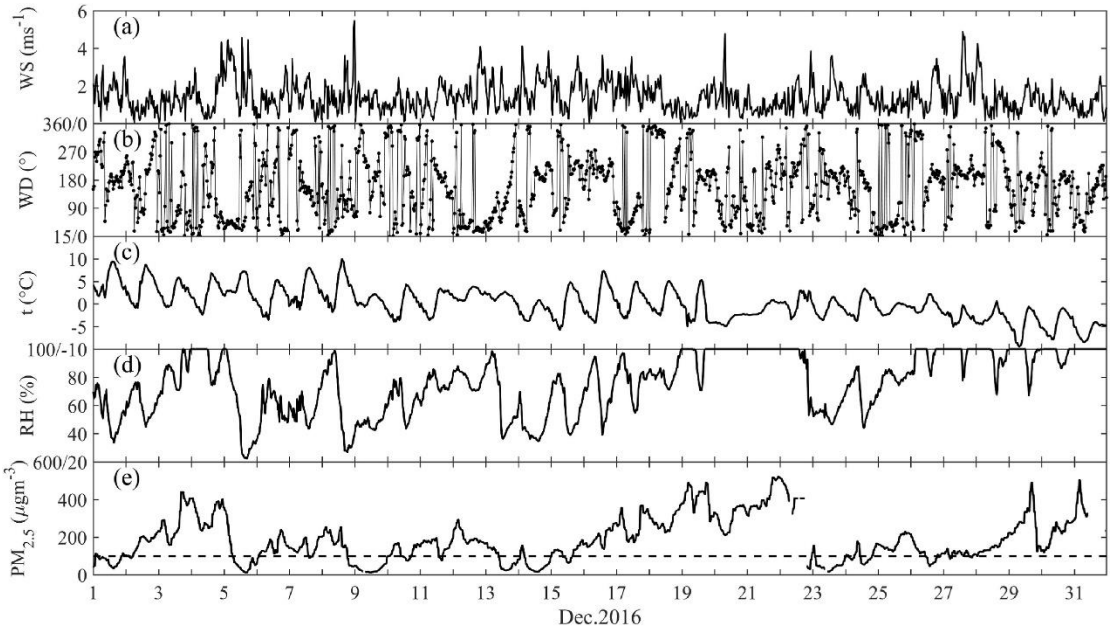

Figure 1. Temporal variations of 4 m (a) surface wind speed, (b) surface wind direction, (c) air temperature, (d) relative humidity, and (e) $PM_{2.5}$ concentration during December 2016. (Cited from Li et al., 2020, Figure 1, underlying surface of wheat fields)

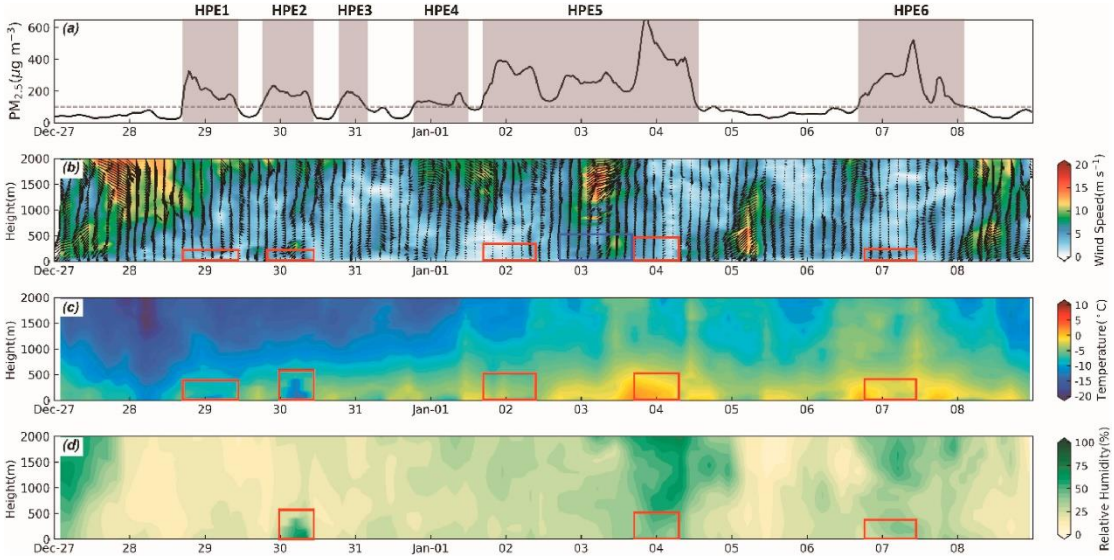

Figure 2. Time series of (a) $PM_{2.5}$ concentrations and time-height cross sections of (b) wind speed, (c) temperature, and (d) relative humidity from sounding data from December 27, 2018, to January 8, 2019. (Cited from Jia et al., 2022, Figure 3, underlying surface of flat farmland)

Furthermore, studies conducted on the underlying surfaces of other cities (Ren et al., 2019a, 2019b) have shown that Beijing and Tianjin city had no consistent haze pollution pattern (see Figure 3a and Figure 4 a1-a2). Additionally, we further analyzed the $PM_{2.5}$ concentration data in the UCL of Lanzhou Basin in winter from December 2023 to February 2024. The subsequent observed haze pollution pattern

characteristics were still consistent with those reported in this study (see Figure 5). These findings reinforce the representativeness of our study, indicating that haze pollution in UCL of Lanzhou Basin has a fixed pattern.

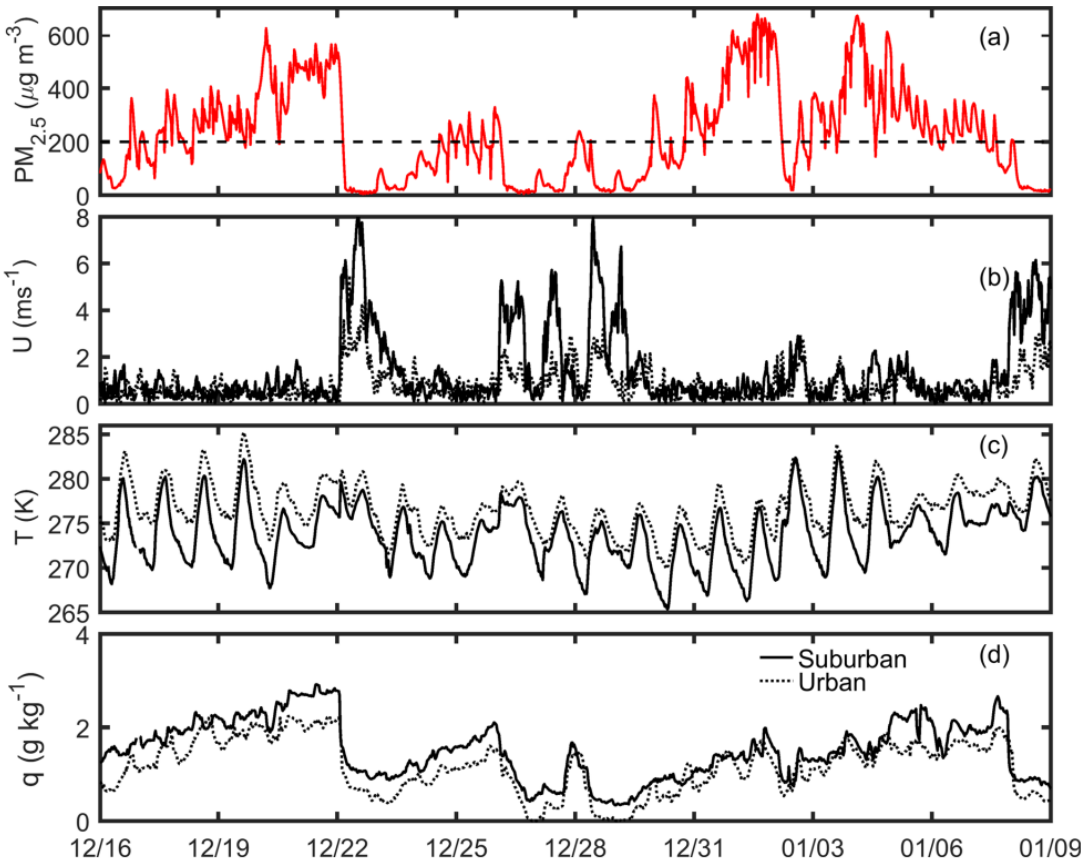

Figure 3. The $PM_{2.5}$ mass concentration (a), horizontal wind speed (b), virtual temperature (c), and water-vapour mixing ratio (d) from 16 December 2016 to 8 January 2017. The black solid line represents data from the suburbs of Beijing (flat terrain), and the black dotted line represents data from the Peking University site (urban landscape). (Cited from Ren et al., 2019a, Figure 3, underlying surface of Beijing city)

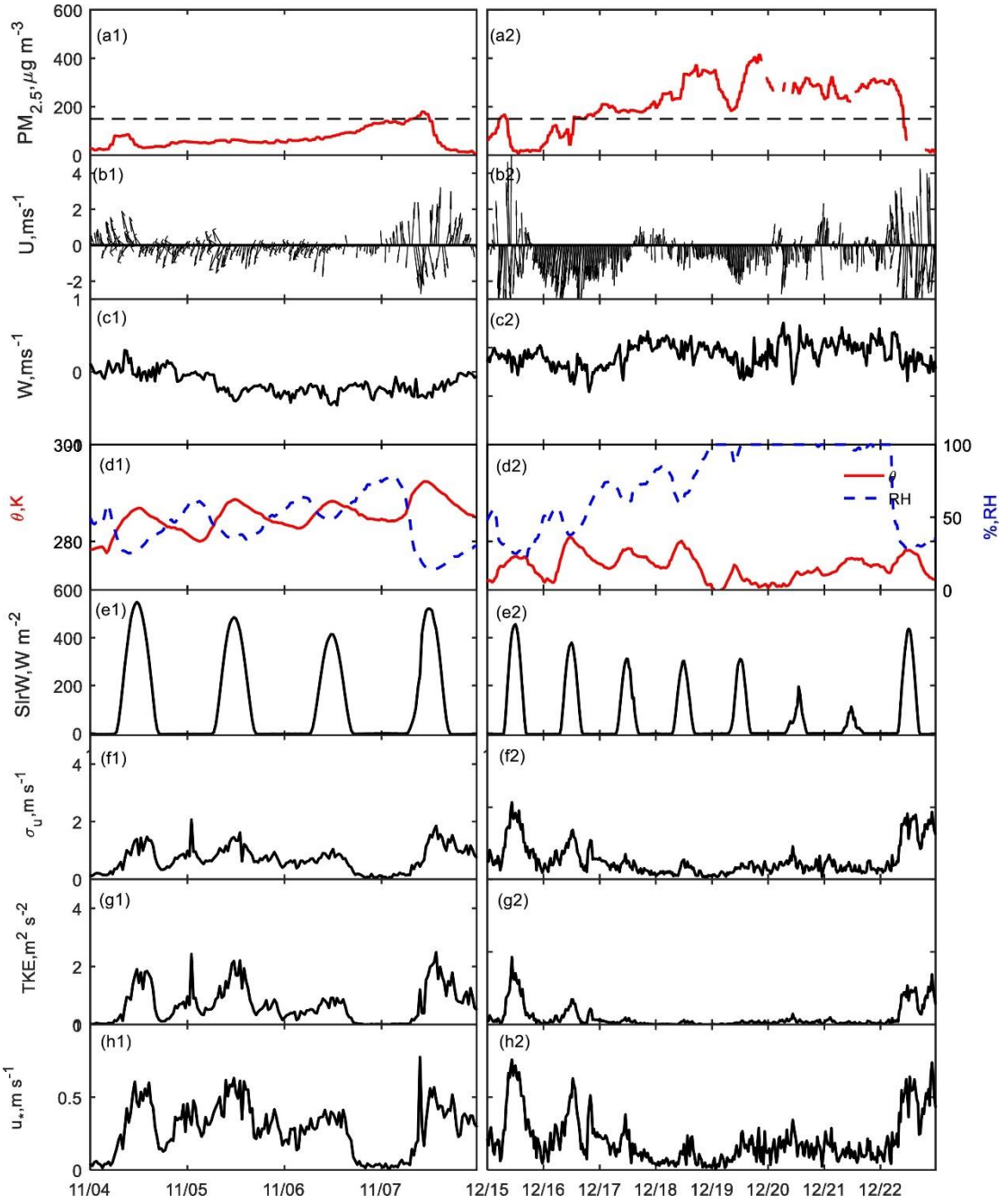

Figure 4. Time series of the $PM_{2.5}$ mass concentration (a1-a2), horizontal wind vector (b1-b2), vertical wind speed (c1-c2), potential temperature and relative humidity (d1-d2), solar shortwave radiation (e1-e2), σ_u (f1-f2), TKE (g1-g2) and u_* (h1-h2). (Cited from Ren et al., 2019b, Figure 6, underlying surface of Tianjin city)

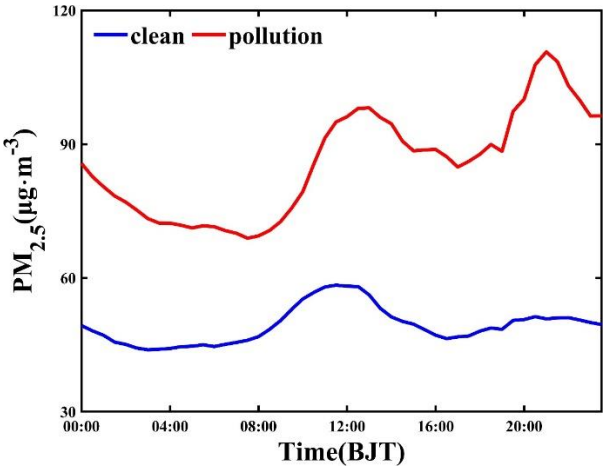

Figure 5. The mean diurnal variation of concentrations of $PM_{2.5}$ under different conditions from the UCL of Lanzhou Basin from December 2023 to February 2024. Solid blue and red lines indicate clean and pollution periods, respectively.

Finally, we will cite these existing studies and provide a detailed introduction to the unique characteristics of the haze pollution pattern in the UCL of basin in Section 3.1 of the manuscript.

2. The authors refer to intermittency as the variation of turbulence intensity, which differs from the traditional definition of intermittency in fluid mechanism. To this reviewer, this is too phenomenological to start with, as quiescent turbulence can be simply related to the decrease in the energy production, instead of sub-mesoscale motions.

Response: Thank you so much for your comments. As stated by Mahrt et al. (2014) "The definition of intermittency varies between studies and disciplines". Mahrt (1999) identified two types of turbulence intermittency: small-scale (or fine-scale) intermittency, which appears as a substructure within the main eddies, and large-scale (or global) intermittency, characterized by aperiodic transitions in both time and space between turbulent and quasi-laminar states, with turbulence locally damped at all scales. Most atmospheric science studies, including this study, focus on global intermittency. This definition has been extensively discussed in numerous classical papers concerning the atmospheric boundary layer (Mahrt, 2010; Mahrt et al., 2014; Acevedo et al. 2014; Sun et al., 2015).

Then, we fully agree with you that the quiescent period of turbulence is indeed related to the decrease in energy production, but during which the influence of sub-mesoscale motions gradually increases. We fully realized the necessity to supplement the details of turbulence intermittency in the original manuscript. We will to introduce the physical mechanisms of turbulence intermittency that we follow below, and then present the theoretical framework for the quantitative characterization of turbulence intermittency here.

(1) The physical mechanisms driving turbulence intermittency

There are several mechanisms that may trigger intermittent turbulence in the atmospheric boundary layer, such as large-scale atmospheric process, surface heterogeneity, the local wind shear, and sub-mesoscale motions. Based on numerous previous studies, mechanisms that trigger turbulence intermittency can be classified into two types: external and internal.

Businger (1973) proposed a theoretical mechanism for the occurrence of turbulence intermittency in the stable boundary layer at night when the sky is clear and cloudless, and this mechanism was verified by Van der Linden et al. (2020) through large-eddy simulation experiments. In particular, at a certain altitude, turbulence weakens or even disappears, and the vertical transfer of momentum and heat is hindered. Thus, above (or below) that altitude, the momentum flux converges (diverges), whereas the wind speed increases (decreases), ultimately increasing the shear. The flow becomes dynamically unstable and turbulence temporarily resumes. The resumption of turbulence causes vertical mixing of momentum and heat and reduction of wind shear. Owing to continuous radiative cooling of the underlying surface, turbulence subsequently weakens and even disappears again. Experimental studies have also found that internal interactions between stable stratification, turbulent mixing, and mean shear can trigger turbulent intermittency (Pardyjak et al., 2002; Fernando, 2003). This type of triggering mechanism is referred to as internal factor for the occurrence of turbulent intermittency (Allouche et al., 2022), and is likely periodic and gives rise to a feedback loop (Van der Linden et al., 2020). The periodic characteristics of turbulence intermittency can be reproduced in large-eddy simulations and non-linear bulk models

(Van de Wiel et al., 2002; Costa et al., 2011; Zhou and Chow, 2014; Van der Linden et al., 2020).

Additionally, turbulence intermittency can also be triggered by sub-mesoscale motions, such as drainage flows (Hiscox et al., 2023), internal gravity waves (Sun et al., 2015), horizontal meandering (Mortarini et al., 2019), and small-scale fronts (Mahrt, 2019). And sub-mesoscale motions are considered as external factors causing turbulence intermittency (Mahrt, 2010a; Sun et al., 2015). Mahrt (2014) defined sub-mesoscale motions as "motions between the primary turbulent eddies and smallest mesoscale motions", which are non-stationary motions. Figure 6a shows the spatial and temporal relationships between sub-mesoscale motions and turbulence motions. Few sub-mesoscale motions can be specifically named, whereas most of them are random disturbances in boundary layers and can only be detected in collected data. Figure 6b shows horizontal meandering motions observed in field experiments.

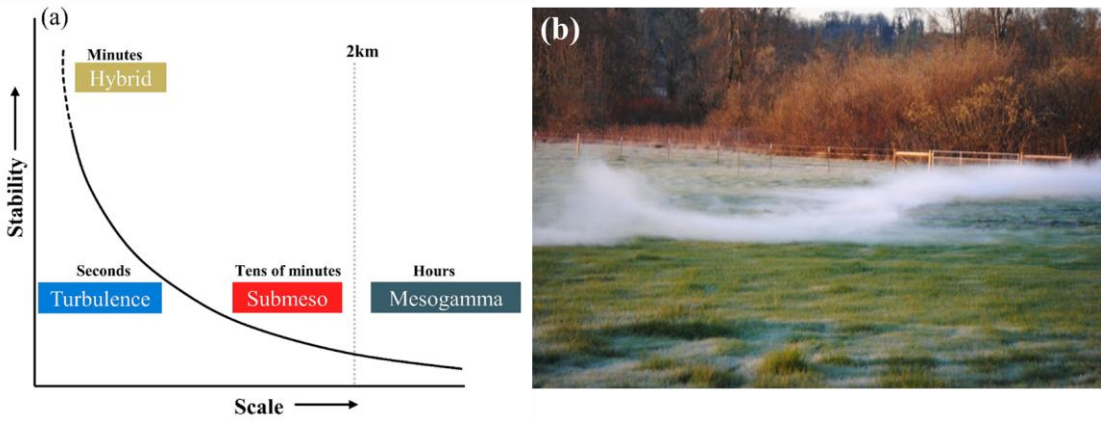

Figure 6. (a) The relationship between the spatiotemporal scales of turbulent motion, hybrid motion, sub-mesoscale motion, and mesoscale motion and atmospheric stability (This figure is revised from Figure 2 of Mahrt (2014)). (b) horizontal meandering motions observed in field experiments. (Cited from www.submeso.org)

(2) Quantitative characterization of turbulence intermittency

Most of the existing methods set thresholds based on intermittent phenomena to characterize turbulence intermittency. For example, a turbulent flux threshold is set for the bursting period to distinguish turbulence intermittency events (Katul et al., 1994). Doran (2004) characterized the intermittency strength through dividing the turbulence duration by the total sampling time. In addition to the time ratio, the flux ratio is also

used to identify turbulence intermittency (Coulter and Doran, 2002). Mahrt (1998) determined the intermittency strength by measuring the degree to which different statistical parameters of turbulence deviate from their average or normal-state values. The methods mentioned above are all based on the manifestations of turbulence intermittency events, which often involve subjectivity and are limited by locality, making it difficult to compare different observation stations.

According to the physical mechanisms driving turbulence intermittency, there exists an additional class of methods to quantitatively characterize turbulence intermittency from the perspective of sub-mesoscale motions. For example, Acevedo and Fitzjarrald (2014) proposed the index R_{sm} to quantify the intensity of turbulent intermittency by using the Multi-Resolution Decomposition (MRD) method. Of course, the limitation of this method is how to quantitatively characterize the sub-mesoscale motion accurately.

Existing methods to separate atmospheric turbulence and sub-mesoscale motions can be classified into two categories. In one type of method, the specific forms of sub-mesoscale motions are considered, aiming to separate certain types of sub-mesoscale motions with prominent characteristics (Román-Cascón et al., 2015; Deb Burman et al., 2018). However, the mid-latitude atmospheric boundary layer is often filled with many different sub-mesoscale motions (Van der Linden et al., 2020; Allouche et al., 2022). The other type of method does not focus on the specific forms of sub-mesoscale motions but on their statistical characteristics under specific conditions (Vickers and Mahrt, 2006; Durden, 2013; Vercauteren et al., 2019). In particular, MRD is the most widely used method of this type. In addition to conventional mathematical analysis, Wei et al. (2016) introduced the Hilbert-Huang transform (HHT) into atmospheric turbulence data analysis, whereas Ren et al. (2019a) developed an algorithm based on the HHT to separate and reconstruct sub-mesoscale and turbulent motions (SMT). The proposed algorithm looks for spectral gaps between large- (weather-scale) and small-scale (turbulence-scale) motions from the Hilbert spectra of observational data, based on which the algorithm subsequently reconstructs the turbulent motion series. Ren et al. (2023) improved SMT algorithm from the perspective of dynamical spectral gap

identification, thereby enhancing the accuracy of the identification of spectral gaps in turbulent fluctuation signals. SMT can help process high frequency pulsation data, any turbulent variable can be separated into two parts, that is, $s' = s'_{turb} + s'_{sub}$, represent turbulent motion and sub-mesoscale motions respectively.

After the successful quantitative characterization of sub-mesoscale motions, some studies have utilized the ratios of turbulence and sub-mesoscale motions in the collected signals to represent the turbulence intermittency strength. Ren et al. (2019a, 2019b) proposed two indices, namely, local intermittent strength of turbulence (LIST) and intermittency strength (IS) to quantitatively characterize turbulence intermittency from the perspectives of kinetic energy of turbulence and sub-mesoscale motions.

Six methods from various perspectives were selected to compare in this recent review, Ren et al., (2025). Figure 7 shows the performance of each method for a turbulence intermittency case and a fully turbulent case, including those proposed by Katul et al. (1994), Doran (2004), Coulter and Doran (2002), Mahrt (1998), Acevedo and Fitzjarrald (2014) and Ren et al. (2023). The different methods and indices show consistency in turbulent intermittency case and fully turbulent case. Furthermore, the indices (LIST and IS) can detect turbulence intermittency events and describe their characteristics, quiescent and burst periods. Additionally, the SMT method and LIST (IS) index have been applied to quantitative turbulence intermittency studies with different types of underlying surfaces, including homogeneous surfaces (Ren et al., 2023), arid complex regions (Wei et al., 2021; Chang et al., 2024), desert hinterland (Zhang et al., 2024), polar regions (Liu et al., 2023), and urban areas (Ren et al., 2019c; Ju et al., 2022; Zhang et al., 2022).

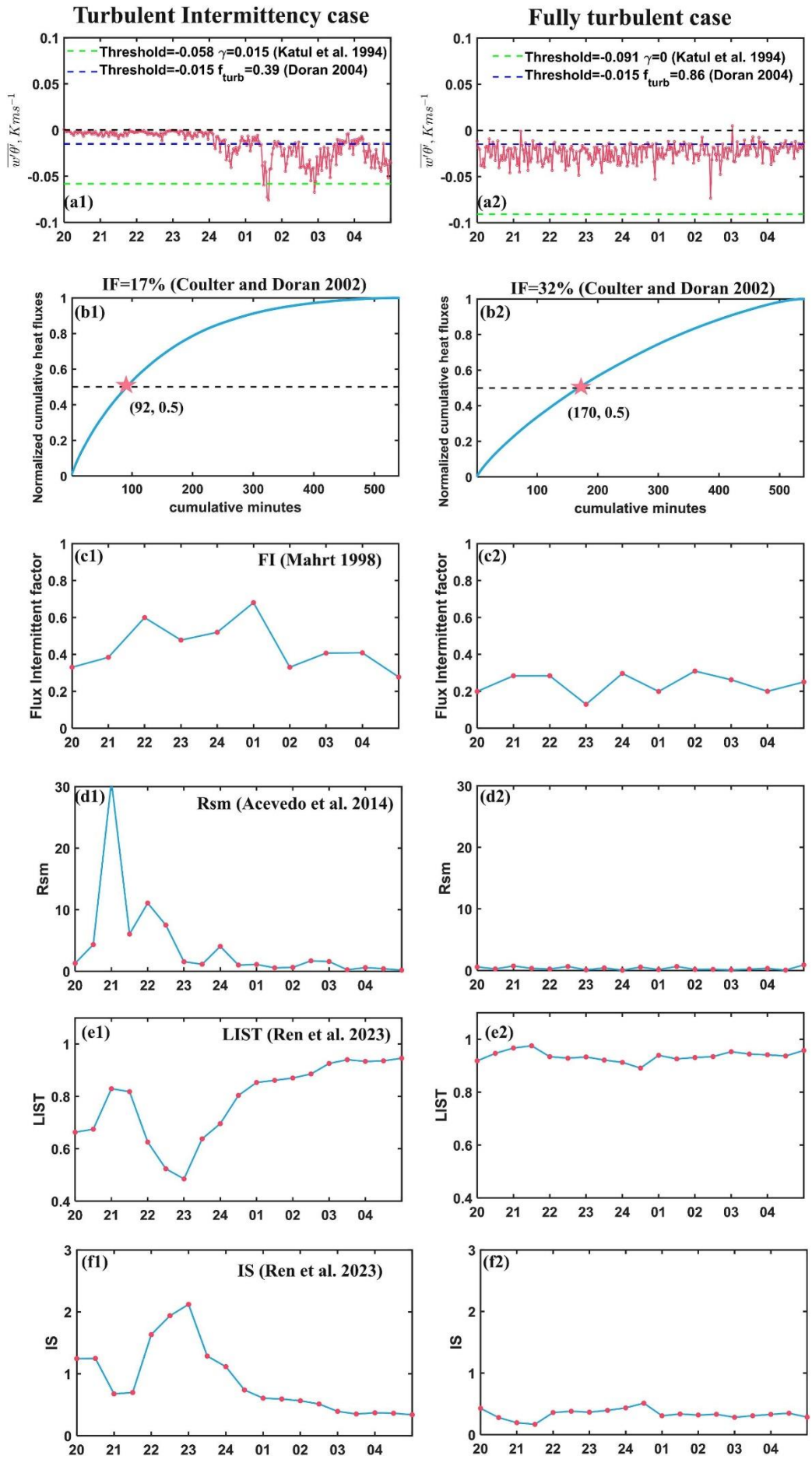
Turbulent Intermittency case
Fully turbulent case
Threshold=-0.058 γ=0.015 (Katul et al. 1994)
Threshold=-0.015 f_turb=0.39 (Doran 2004)
Threshold=-0.091 γ=0 (Katul et al. 1994)
Threshold=-0.015 f_turb=0.86 (Doran 2004)
(a1)
(a2)
IF=17% (Coulter and Doran 2002)
IF=32% (Coulter and Doran 2002)
(92, 0.5)
(170, 0.5)
Normalized cumulative heat fluxes
cumulative minutes
(b1)
(b2)
(c1)
FI (Mahrt 1998)
(c2)
Flux Intermittent factor
(d1)
Rsm (Acevedo et al. 2014)
(d2)
Rsm
(e1)
LIST (Ren et al. 2023)
(e2)
LIST
(f1)
IS (Ren et al. 2023)
(f2)
IS

Figure 7. Different indexes characterizing turbulence intermittency in intermittency case and pure turbulent case. (Cited from Ren et al., 2025, Figure 6)

Finally, thanks again for your comments. We realized that our initial description of turbulence intermittency in the original manuscript was insufficient. Therefore, we intend to supplement the definition and the physical mechanisms of turbulence intermittency that we follow, and then present the theoretical framework for the quantitative characterization of turbulence intermittency in the introduction and methods section of manuscript.

3. The partition of sub-mesoscale motions and turbulence motions is artificial and lack theoretical basis. This might be true in some specific situations, e.g., the gradient Richardson number exceeds 0.25, as waves can survive and turbulence is not influenced by the wall. However, in neutral and unstable boundary layers, waves are dynamically unstable and will definitely break into turbulence. Given that large scale turbulence is anisotropic in neutral and unstable boundary layers, the scales beyond the plateau in energy spectrum could be still turbulence, see relevant works by Marusic.

Response: Thank you for your helpful comments and recommendations. We fully agree with the importance of theoretical basis, and we have read the relevant works by Marusic, which have greatly enhanced our understanding of fluid dynamics. Our study followed the well-established theoretical framework of sub-mesoscale motions and turbulence motions in atmospheric boundary layer turbulence (Mahrt 2009, 2014; Acevedo et al. 2014), primarily encompassing the following aspects:

Mahrt (2014) defined sub-mesoscale motions as “motions between the primary turbulent eddies and smallest mesoscale motions”. Sub-mesoscale motions include drainage flows, horizontal meandering, internal gravity waves, “dirty waves”, among others.

Distinct spectral gaps have been detected in energy spectra of turbulence quantities in many studies with the help of different mathematical tools (Muschinski et al., 2004; Vickers and Mahrt, 2003). To decompose turbulent and sub-mesoscale parts in the

observed fluctuations, spectral approaches are usually adopted, on the basis of the appearance of spectral gaps between turbulence and sub-mesoscale motions (Mahrt, 2007; Wei et al. 2017; Mahrt and Bouzeid, 2020). Common spectral analysis methods include wavelet analysis (Salmond 2005), multi-resolution decomposition (MRD; Vickers and Mahrt 2003; Acevedo et al. 2014) and Hilbert–Huang transform (HHT; Huang et al. 2008; Wei et al. 2017), where the latter appears to be superior since it is fully data driven. Vickers and Mahrt (2003) employed the method of MRD to study the turbulence intermittency. Their findings revealed obvious spectral gaps between the turbulence scale and the sub-mesoscale motions. Specifically, the momentum fluxes and heat fluxes exhibited an increase over time within scales smaller than the spectral gaps. Conversely, in timescales longer than the spectral gaps, their variability rosed, as illustrated in Figure 8. Ren et al. (2019a) developed an algorithm based on the HHT to separate and reconstruct sub-mesoscale and turbulent motions (SMT). The proposed algorithm looks for spectral gaps between large- (weather-scale) and small-scale (turbulence-scale) motions from the Hilbert spectra of observational data, based on which the algorithm subsequently reconstructs the turbulent motion series. In the second-order Hilbert spectra (see Figure 9), we can clearly observe the significant spectral gaps. The right sides of these spectral gaps aligned with the expectations of classical energy spectrum theory, whereas the left sides showed deviations from these expectations. Similarly, the study of Liu et al. (2023) also explored the application of spectral gaps in distinguishing sub-mesoscale motions from turbulent motions, as shown in Figure 10. Zhang et al. (2024) even directly considered the energy at the position of the spectral gap as a sub-mesoscale motion. Furthermore, Ren et al. (2023) improved SMT algorithm from the perspective of dynamical spectral gap identification, thereby enhancing the accuracy of the identification of spectral gaps in turbulent fluctuation signals (see Figure 11). SMT can help process high frequency pulsation data, any turbulent variable can be separated into two parts, that is, $s' = s'_{turb} + s'_{sub}$, represent turbulent motion and sub-mesoscale motions respectively. Nevertheless, on some occasions, there are no clear spectral gaps but instead an intermediate scale range characterized by the superposition of turbulence and sub-mesoscale motions, called

hybrid motions (Mahrt 2014).

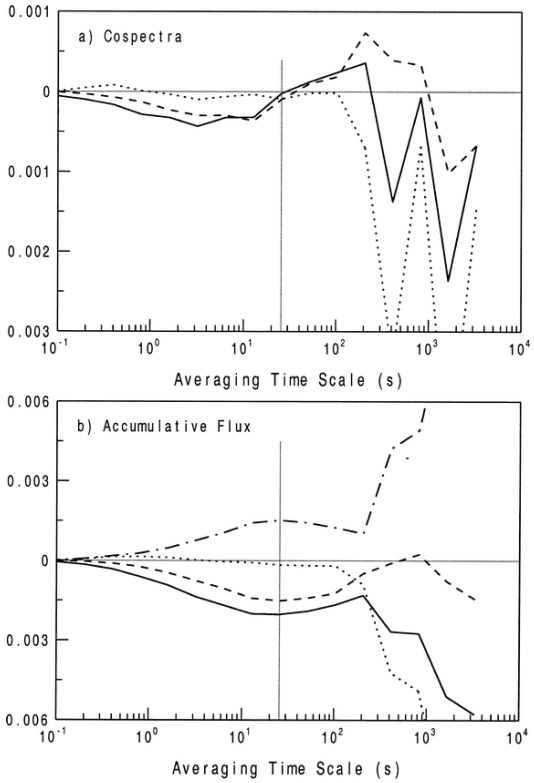

Figure 8. 5-m sonic data for one stable period around midnight for the sonic heat flux (solid line), along wind component of momentum flux (dash), crosswind momentum flux (dots), and magnitude of momentum flux [dash–dot; (b) only] for (a) the co-spectra, and (b) the accumulative flux. Vertical line is the gap time scale detected by the algorithm (26 s). (Cited from Vickers and Mahrt 2003, Figure 4)

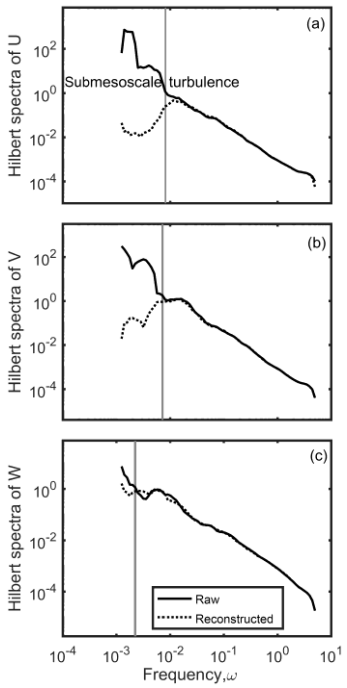

Figure 9. Second-order Hilbert spectra of three wind speed components U (a), V (b), and W (c) at

08:00 on 31 December 2016 at the suburban site. The black solid line indicates the spectra from the raw data, and the black dotted line indicates the spectra from the reconstructed data for pure turbulence. The solid gray lines indicate the position of the spectral gap. (Cited from Ren et al., 2019a, Figure 3)

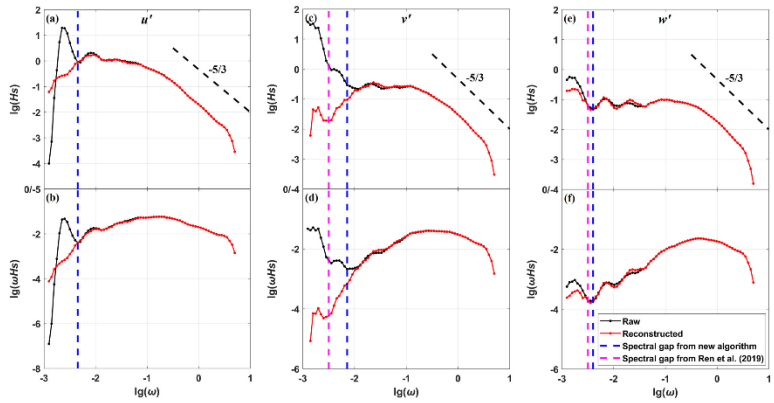

Figure 10. The second-order Hilbert spectra of three wind speed components u′ (a, b), v′ (c, d), and w′ (e, f) at 09:30 on 10 November 2019. The upper panels show the spectra of Hs, while the lower panels show the spectra of ωHs. The magenta and blue dashed lines indicate the locations of the spectral gap identified by Ren et al. (2019a) and our new algorithm, respectively. The solid black lines are the spectra from raw data, and the solid red lines represent the spectra from reconstructed data for pure turbulence according to the spectral gap identified by our new algorithm. (Cited from Liu et al., 2023, Figure 4)

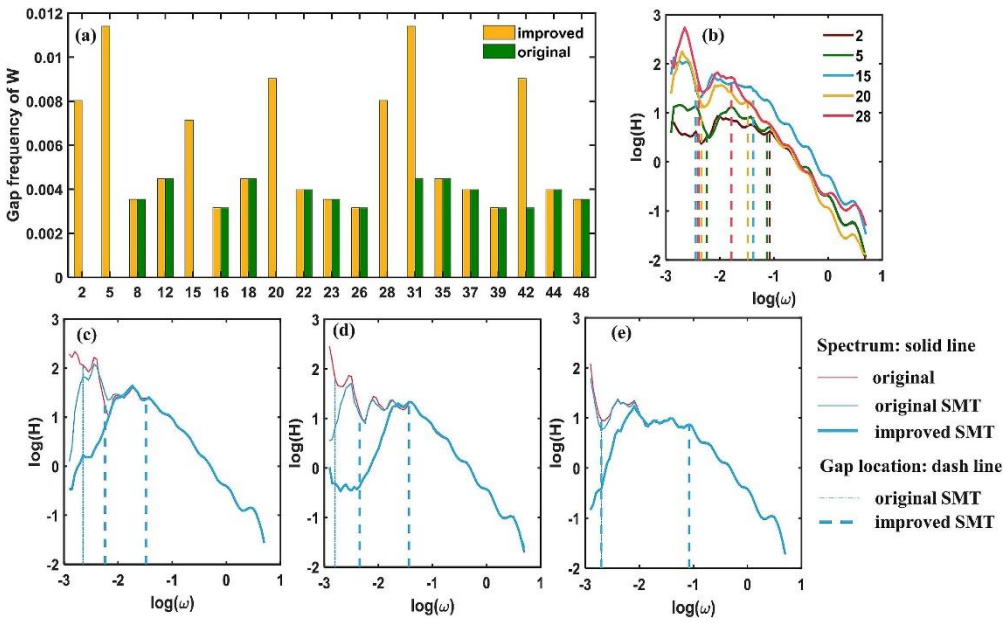

Figure 11. The gap frequency of vertical wind speeds determined by improved (yellow) and original (green) SMT (a). The spectra of five groups of data (b). The original and reconstructed spectra of these two data sets: 31 (c) and 42 (d). The original and reconstructed spectra of a case with same gap frequency in both methods (d). The solid pink line represents the spectrum of the original data. The bold blue line represents the reconstructed spectrum of improved SMT. The thin blue line represents he reconstructed spectrum of original SMT. The dotted line marks the location

of the spectral gap. (Cited from Ren et al., 2023, Figure 2)

Through observation experiments conducted on both complex and flat terrains, Anfossi et al. (2005) found that meandering seems to exist under all meteorological conditions regardless of the stability or wind speed. Meandering is one kind of sub-mesoscale motions (Mortarini et al., 2019). Mahrt (2014) also mentioned that although sub-mesoscale motions seem to always be present, their impact is limited primarily to weak-wind conditions. Furthermore, Mahrt (2010b) pointed out that the non-stationary conditions include boundary-layer transitions, most stable boundary layers and most weak-wind unstable boundary layers. Thus, beside the very stable boundary layers, turbulence in the weak-wind unstable boundary layers may intermittent as well due to sub-mesoscale motions. Zhang et al. (2024) and Wei et al. (2021) both discussed the effects of the presence of sub-mesoscale motions on the turbulent transport in the unstable boundary layer (see Figure 12). However, we fully concur with your perspective. We consider that although sub-mesoscale motions are present during daytime, their intensity is weaker compared to nocturnal conditions. And they are more likely to be triggered by the complex underlying surfaces.

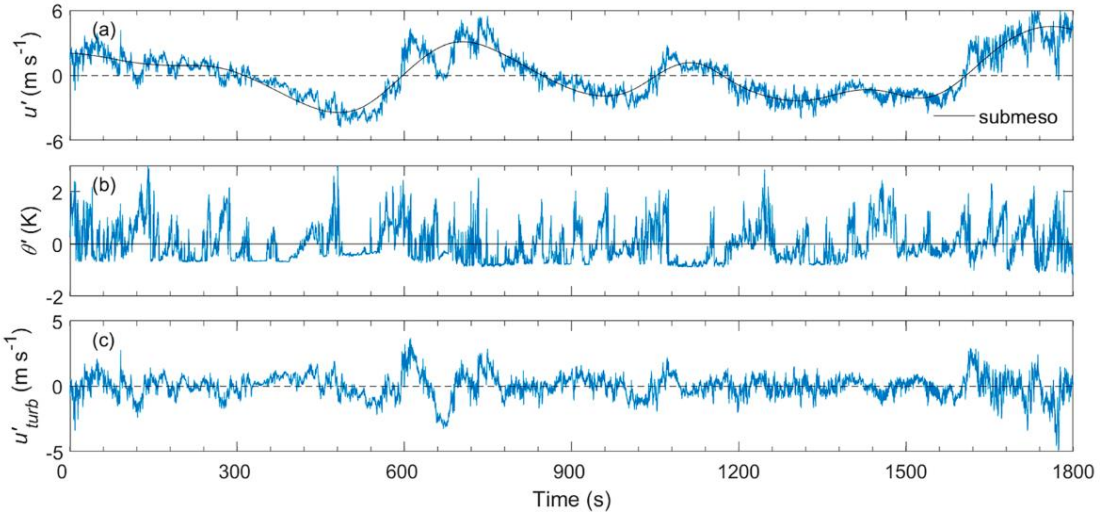

Figure 12. Time series of original (a) u′, (b) original/turbulent θ', and (c) turbulent u′ for the selected 30-min segment under strongly unstable conditions. The black lines in (a) represent the fluctuations induced by the horizontal convergence/divergence of convective circulations (sub-mesoscale motions). (Cited from Zhang et al., 2024, Figure 7)

Our field experiments conducted in the UCL, where the underlying surface is

highly complex and wind speeds are relatively weak. The development of turbulent eddies within the UCL can be easily constrained or fragmented by roughness elements. And haze pollution often occurs in weak wind conditions (see Figure 13). Both the complex underlying surface and the weak wind are consistent with the conditions for the occurrence of sub-mesoscale motions in the literatures. Moreover, our observations have also found the non-turbulent feature of "dirty waves" in the UCL. It can be seen from Figure 14 that original u′, v′, and w′ are all characterized by distinct wavelike signals. The amplitude and period of waves vary between cycles, which is referred to as "dirty waves" (Mahrt 2014; Cava et al. 2015). The separated sub-mesoscale signals of u′, v′, and w′ (i.e., black lines in Figure 14a–c) follow the "dirty waves" well, which means the sub-mesoscale motions represent as "dirty waves" in the UCL.

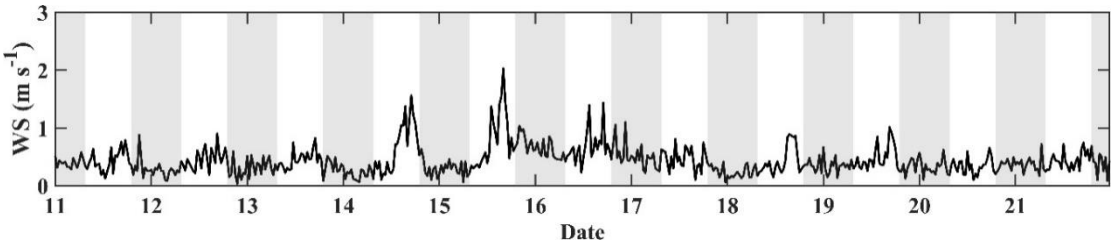

Figure 13. Time series of horizontal wind speed (WS) from January 11 to 21, 2021. The gray shading represents night between 19:00 and 07:00 the following day.

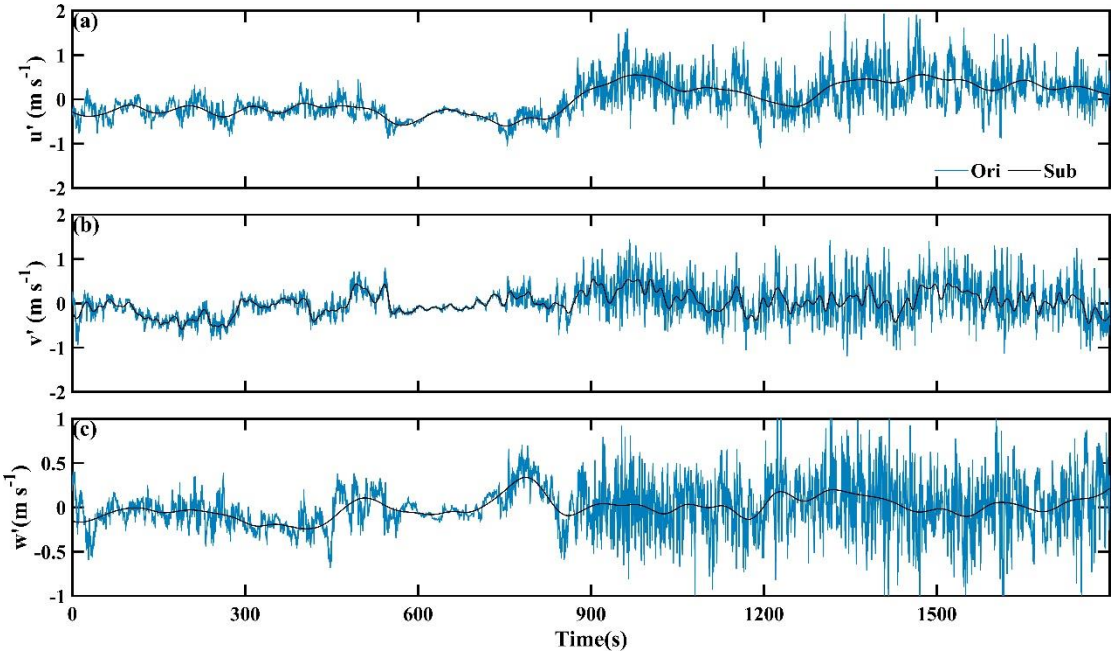

Figure 14. Time series of original (a) u′, (b) v′, and (c) w′ for the selected 30-min segment in the UCL of basin. The black solid lines represent the fluctuations induced by sub-mesoscale motions.

Thanks again for your valuable comments. We follow the theoretical framework of sub-mesoscale motions in existing studies. Due to the constraints of the complex urban terrain, our actual observations found non-turbulent disturbances in high frequency signals. We are sorry that we failed to explain it clearly in the original manuscript. We will emphasize the definition and quantitative characterization of sub-mesoscale motions in the introduction section of the original manuscript. Additionally, we further supplement the details and theoretical basis of the methods used in the methods section, as well as incorporate examples of sub-mesoscale motions observed in the UCL (Figure 14).

4. As the observations are collected within the canopy layer, the observed fluid motions must be local, the authors have to prove that there are sub-mesoscale motions in UCL and they are important.

Response: Thank you for your insightful comments on turbulence characteristics within the UCL. We fully concur that the fluid motions observed in UCL must be local. In the last response, we introduced the definition of sub-meso scale motions we follow, the quantitative characterization theory framework we follow, and showed a case of "dirty waves" in Figure 14. We think we must be clear about this now.

Multiple observational studies have demonstrated that sub-mesoscale motions are site dependent and tend to be greater in complex terrain (Anfossi et al., 2005; Vickers and Mahrt, 2007; Wei et al., 2021; Zhang et al., 2024). Wei et al. (2021) and Zhang et al., (2024) analyzed the characteristics of the turbulence intermittency and its influence on the complex terrains, they also found that sub-mesoscale motions can occur during the daytime. In our study, we used the SMT algorithm to identify the spectral gaps in 1488 groups of 10 Hz high-frequency data from January 2021 within UCL. Specifically, there are 1090 (73%), 1089 (73%), and 893 (60%) groups of data in the along-wind direction u, the cross-wind direction v, and vertical direction w, respectively. In addition, the spectral gaps identified in our study are presented (see Figure 15). Therefore, our study observed sub-mesoscale motions under the same conditions described in reported studies: complex terrains and weak winds. The observed non-turbulent motions of

"dirty wave" in high-frequency fluctuations also match existing studies (Zhang et al., 2024).

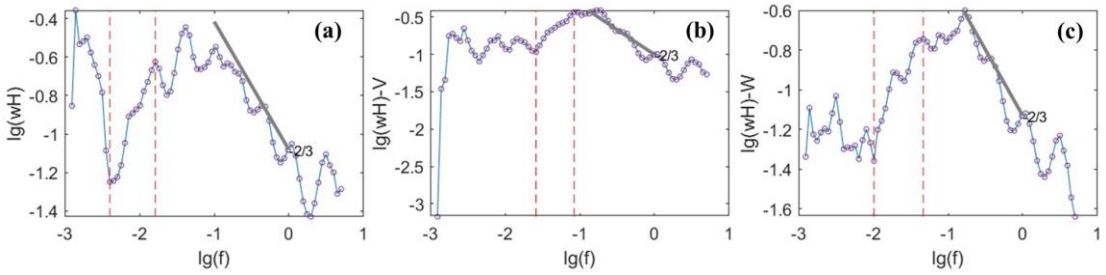

Figure 15. Second-order Hilbert spectra of three wind speed components u (a), v (b), and w (c) for the selected 30-min segments in the UCL (the time is the same as in Figure 14), respectively. The two red dashed lines indicate the range of the spectral gap.

Thanks again for your helpful comments. We realize that the introduction of sub-mesoscale motions in the original manuscript was inadequate, potentially causing confusion for readers from diverse backgrounds. To address this issue, we plan to emphasize the definitions of sub-mesoscale motions and turbulent motions, the law of the spectral gap between sub-mesoscale motions and turbulent motions, and the literatures about sub-mesoscale motions occurring conditions in the introduction section. Furthermore, in the method section, we would like to describe detailly the theoretical basis of partition of sub-mesoscale motions and turbulence motions, and supplement the frequency of the occurrence of spectral gaps and the forms of sub-mesoscale motions (Figure 14 and Figure15) found in the UCL.

5. The observed haze pollution pattern can be simply explained as: (1) The decrease of $PM_{2.5}$ from 00:00 to 08:00 is due to the decrease in the emission according to Fig. 2b; (2) The increase of $PM_{2.5}$ from 08:00 to 14:00 is due to the increase in the emission according to Fig. 2b; (3) The decrease of $PM_{2.5}$ from 14:00 to 18:00 is due to the strengthening turbulence by unstable stratification according to Fig. 2f, 2i; (4) The increase of $PM_{2.5}$ from 18:00 to 00:00 is due to the suppressed turbulence by stable stratification according to Fig. 2f, 2i.

Response: Thank you for your constructive comments. We fully agree with that the haze pollution pattern is related to emission intensity and atmospheric stratification. In

addition, an interesting finding in our study is that the source emission intensity was weaker during the haze pollution periods compared to the clean periods, yet haze pollution still formed within the UCL of basin. This suggested that meteorological conditions might play a crucial role in the process of haze pollution. During the haze pollution periods, we observed lower relative humidity and horizontal wind speed (see Figure 16c and Figure 16e), but higher near-surface temperature (see Figure 16d). Previous studies indicated that higher relative humidity would promote the hygroscopic growth of fine particulate matters (Quan et al., 2011; Chen et al., 2012), while higher near-surface temperature supposed the development of unstable stratification. These characteristics of relative humidity and temperature were unfavorable to the formation of haze pollution, and it seemed difficult to discuss clearly the decisive contribution of these local meteorological conditions. Therefore, we continue to study the impact of turbulence in the UCL.

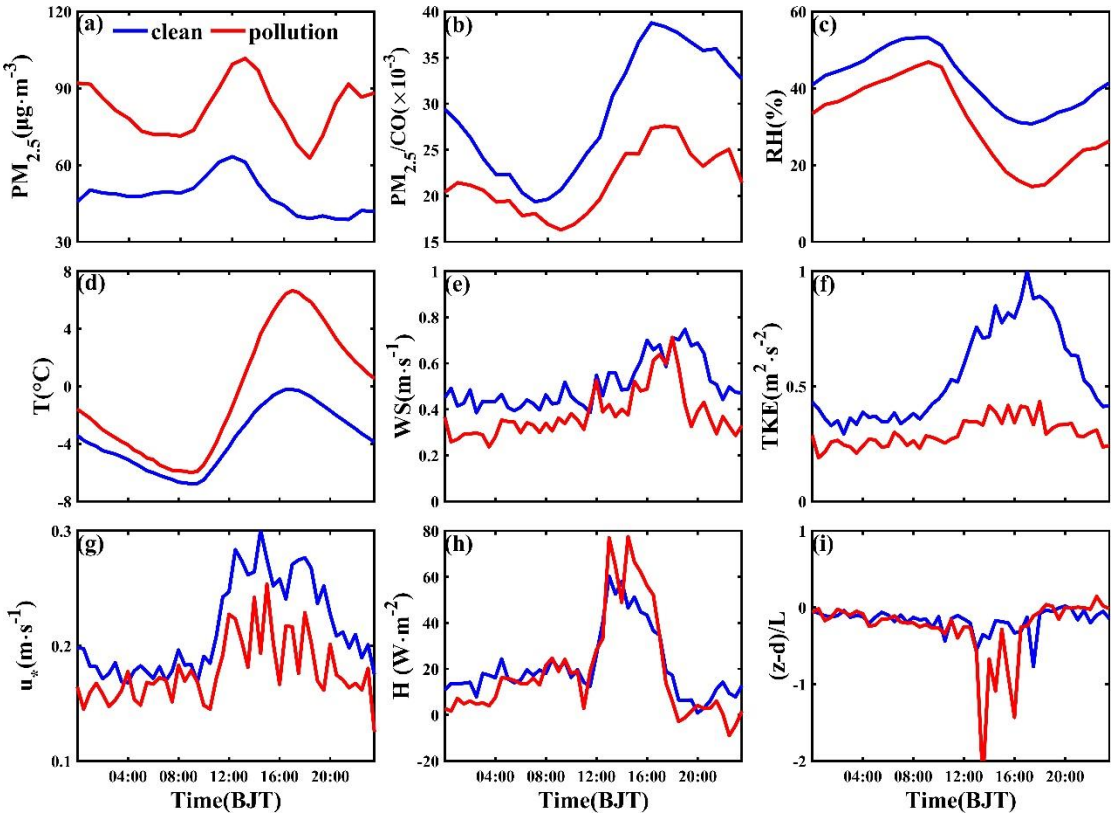

Figure 16. The mean diurnal variation of (a) concentrations of $PM_{2.5}$, (b) $PM_{2.5}$/CO, (c) relative humidity (RH), (d) temperature (T), (e) horizontal wind speed (WS), (f) turbulent kinetic energy (TKE), (g) friction velocity (u_*), (h) sensible heat flux (H), and (i) stability parameter ((z-d)/L) under different conditions from LACMS in January 2021. Solid blue and red lines indicate clean and pollution periods, respectively. (From original manuscript Figure2)

This unique distinctive haze pollution pattern is not only associated with emission intensity and atmospheric stratification, but also influenced by the multi-scale turbulent structures in the UCL of basin. In addition, we also found that the turbulent structure characteristics in the UCL of basin differ significantly from those in plain cities (Ren et al., 2019a; Wang et al., 2020). Specifically, the sensible heat flux reduced and the atmospheric stratification was more stable during haze pollution periods (see Figure 17a and 17e). However, the observations of our studies indicated that the sensible heat flux was greater and the atmospheric instability was stronger during haze pollution periods, which may be attributed to the stronger influence of human activities. (see Figure 16h and Figure 16i)

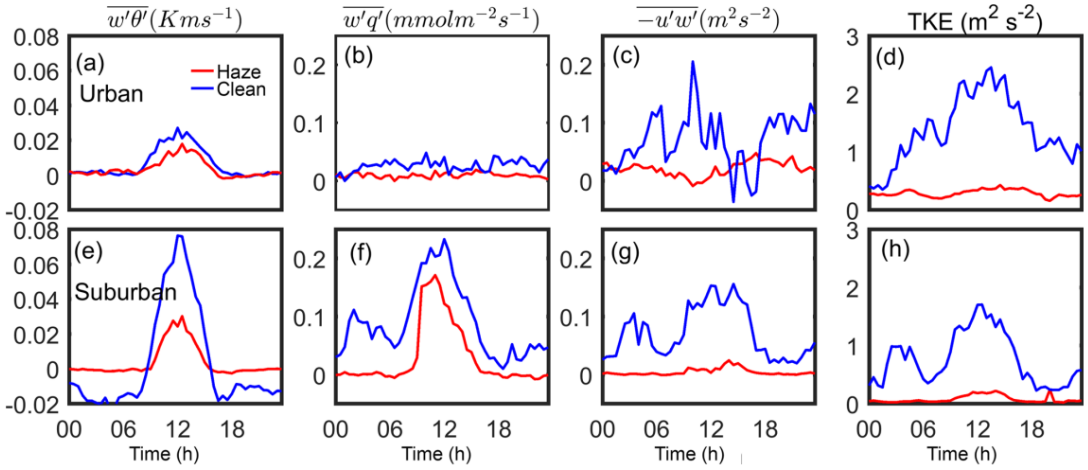

Figure 17. Diurnal variations in the mean vertical heat flux (a), vertical water-vapour flux (b), momentum flux (c), and TKE (d) under polluted weather (red solid line) and clear weather (blue solid line) conditions over the urban site. Diurnal variations in these variables over the suburban site are shown in (e), (f), (g), and (h). (Cited from Ren et al., 2019a, Figure 11)

The atmospheric turbulence structure of the UCL in the basin is highly complicated and characterized by strong non-stationarity and inhomogeneity due to the influence of the heterogeneous distribution of rough elements and human activities. The Monin–Obukhov similarity theory serves as a critical theoretical framework for measurement and analysis in the fields of atmospheric boundary layer and atmospheric turbulence research. And it is the basis for parameterization of turbulence in the atmospheric boundary layer for air pollution prediction, numerical weather forecasting, and climate modeling. Strictly speaking, Monin–Obukhov similarity theory only

applies to stationary and homogeneous turbulence; thus, the applicability of similarity theory within the UCL is questionable (Roth, 2000; Zou et al., 2015). Our detailed analysis reveals how the complex multi-scale turbulence structures in the UCL of basin influence the both occurrence and evolution of haze pollution events. These findings can provide substantial observational basis and theoretical support for improving the boundary layer parameterization schemes in the urban air quality forecast models.

Finally, we sincerely thank you for constructive comments, which are very extremely beneficial to our study. We intend to supplement the description of the difference in haze pollution pattern within the UCL of basin compared to other cities and various underlying surfaces in Section 3.1. Additionally, we will provide a clearer explanation of the unique turbulence structure present in the UCL.

6. Fig. 4a should move to method section.

Response: Thank you for your helpful comments. We will move Figure 4a to method section in the manuscript.

7. The review does not see the necessity of the discussion on the time scale of turbulence in Sect. 3.2. For one thing, 15-min scales on 20 Jan also contributes significantly to TKE, but why $PM_{2.5}$ is less changed?

Response: Thank you for your valuable comments. Figure 18 illustrates the multi-resolution decomposition (MRD) spectra of TKE in different time scales on January 20. The MRD allows comparing the TKE contribution from each range of time scales, especially in the turbulent (smaller) scales. The time series of the $PM_{2.5}$ concentration (white lines) and the total TKE (as the sum of the contribution from all scales up to 30 min, black line) are included in the Figure 18, as well as the filled colors represent the spectral values of TKE on different time scales. It can be seen from Figure 18 that the eddy scale significantly contributes to TKE was greater than 15 minutes at 13:00 on January 20, but the $PM_{2.5}$ concentration was less changed at this time. When the eddy scale was less than 15 min at 14:00, the $PM_{2.5}$ concentration began to decrease. During the period from 14:00 to 17:00, the eddy scale that significantly contributed to TKE

mainly remained smaller than 15 min, $PM_{2.5}$ was also on the decline.

These findings, observed on January 20, were consistent with other dates. They were also consistent with our conclusions that small scale eddies with time scale shorter than 15 min or even 2 min from 14:00 to 18:00 can efficiently remove fine particle matters, resulting in the reduction of $PM_{2.5}$ concentrations.

Finally, thank you again for your comments. we acknowledge this wasn't sufficiently clear in the original manuscript, and we will supplement these detailed analyses in Section 3.2.

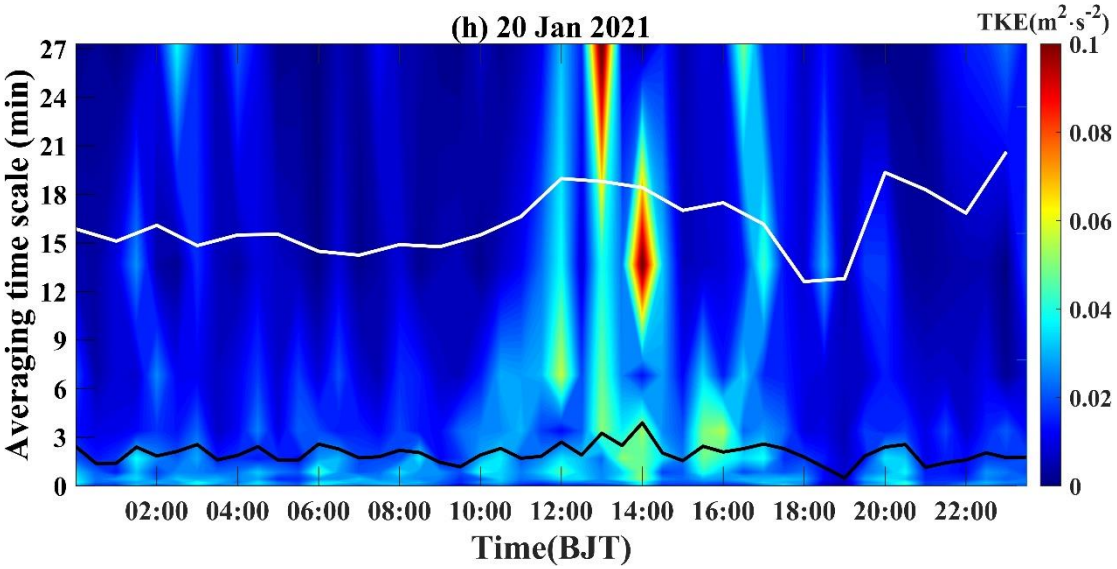

Figure 18. Multi-Resolution Decomposition (MRD) spectra of turbulent kinetic energy (TKE) for January 20 over 30 min time scales. The solid black and white lines represent TKE average values within 30 min and the $PM_{2.5}$ concentrations, respectively, and the filled colour denotes the TKE spectrum values.

8. "Acevedo et al. (2014) found that TKE increased exponentially with the time scale in the sub-mesoscale motions range. Fig. 3 showed that when the eddy scale exceeded a certain threshold (e.g., 15 min), the TKE spectral value increased with the timescale. That suggested the presence of sub-mesoscale motions in this situation." Why does this follow logically? At the first place, the increase of TKE spectral value with timescale does not necessarily indicate the presence of sub-mesoscales. Secondly, the reviewer does not see the increase of TKE spectral value in Fig. 3.

Response: Thank you for your helpful comments. Vickers and Mahrt (2006) developed

a multiresolution decomposition (MRD) method to separate the turbulent and sub-mesoscale motions based on multiresolution co-spectra. Acevedo et al. (2014) also used the same method to identify the contributions of sub-mesoscale motions to spectra from six different observation sites. They found that turbulent kinetic energy increased exponentially with the time scale in the sub-mesoscale range, and the increased rate was larger under weak turbulence situations (see Figure 19).

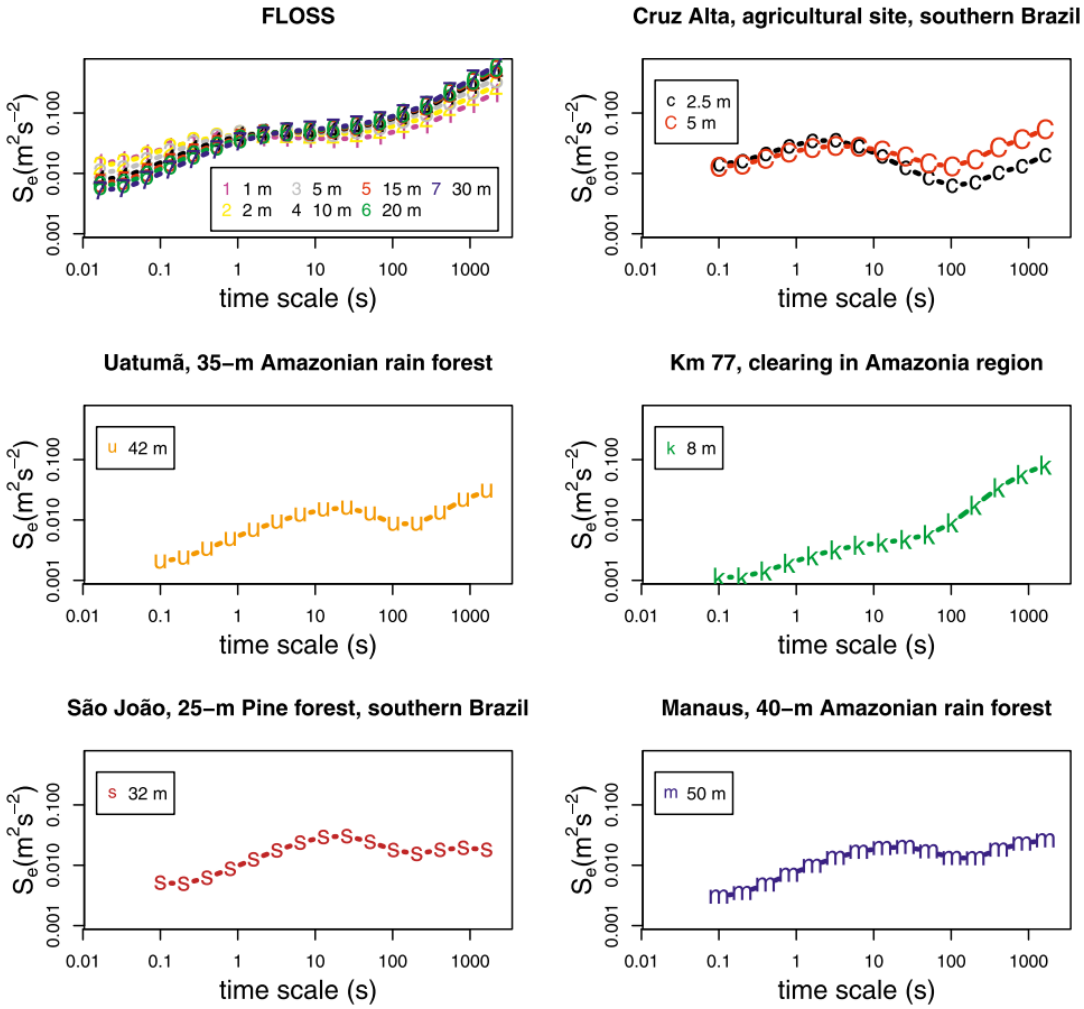

Figure 19. Average TKE spectra for each site and each level, according to legend. (Cited from Acevedo et al., 2014, Figure 1)

Similarly, we also employed the method developed by Acevedo et al. (2014) to identify the contributions of sub-mesoscale motions to spectra. And we selected three specific cases (12th 15:30, 12th 19:00 and 17th 15:00), as illustrated in Figure 20. It can also be seen from Figure 20 that the sub-mesoscale motions increased exponentially over their time scale. Although our data was a half-hour average, it aligned with the

average conditions described by Acevedo et al. (2014). A feature observed in the filling color representation of the TKE spectrum in our study was that when exceeding a certain time scale (e.g., 15 min), there was a continuous deepening of color became red as the time scale increased. This trend indicated that the sub-mesoscale motions increased with the time scale, such as those recorded 12th at both 15:30 and 19:00, as well as on the 17th at 15:00 (in the white box of Figure 21).

We sincerely apologize for the vagueness, which stemmed from a lack of clarity in our original manuscript. To address this issue, we will supplement more details in Section 3.2.

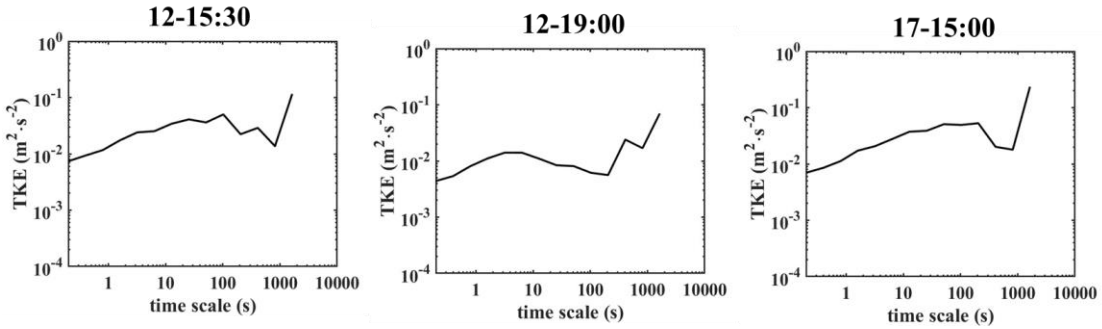

Figure 20. TKE spectra in the UCL of basin at 15:30,19:00 on the 12th and 15:00 on the 17th.

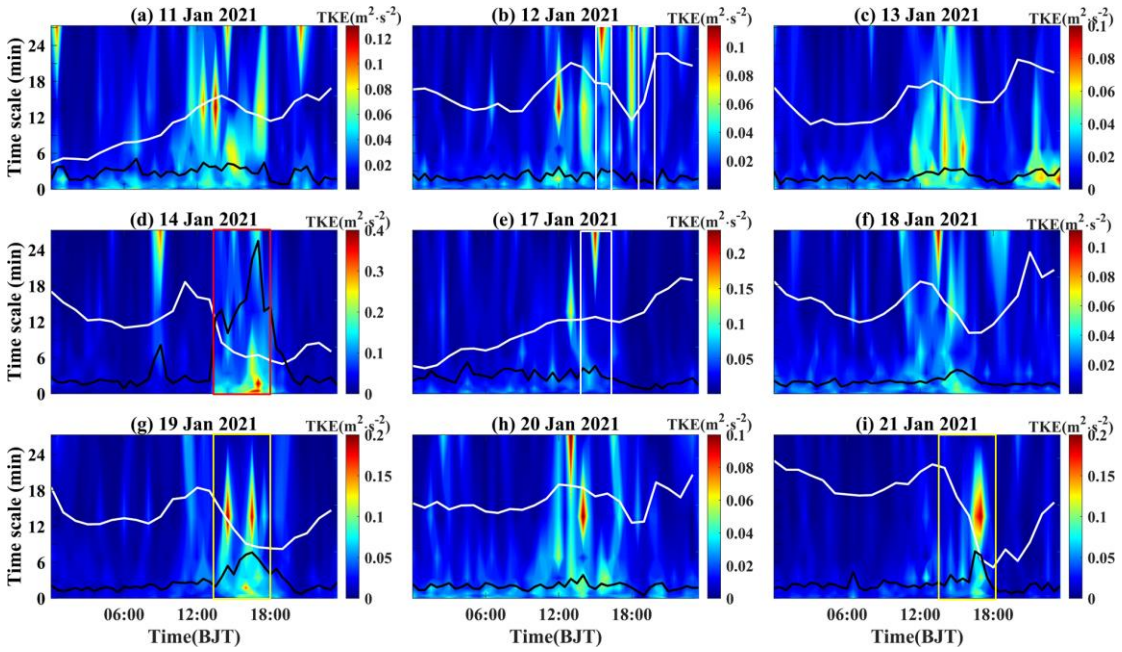

Figure 21. Multi-Resolution Decomposition (MRD) spectra of turbulent kinetic energy (TKE) for Case 1 (January 11–14, 2021, a-d) and Case 2 (January 17–21, 2021, e-i) over 30 min time scales. The solid black and white lines represent TKE average values within 30 min and the $PM_{2.5}$

concentrations, respectively, and the filled colour denotes the TKE spectrum values. (From original manuscript Figure3)

9. Consequently, the discussion on \delta KE in Page 13 is of less interests. The authors should plot spontaneous velocities to see whether sub-mesoscale motions emerge.

Response: Thank you for your valuable comments. According to the introduction of existing literatures and the actual observation results in this study, the sub-mesoscale motions indeed appear in the UCL of basin, and there also exists the energy transition between sub-mesoscale motions and turbulent motions.

10. Page 14 Lines 2-5: do the authors mean that sub-mesoscales are more efficient in mixing than turbulence by this sentence?

Response: Thank you for your valuable comments. In fact, turbulent mixing was more efficient in most cases of our study.

During 00:00-07:00 on January 14, 2021, there was only one case where the sub-mesoscale motions were relatively stronger, yet it corresponded to a decrease of $PM_{2.5}$ concentration. This period was in weak wind conditions with high turbulence intermittency intensity (wind speed can see from Figure 13). We didn't assert that sub-mesoscale motions were more efficient in mixing than turbulence. In fact, turbulent mixing was more efficient in most other cases (Figure 22). The horizontal wind speeds and the turbulence intensity at night on other days were lower, while the LIST gradually increased (such as nights of the 12th and 13th). Which indicated that the short-term turbulent bursts might break the turbulent barrier of the layer and promote the transfer and exchange of substances, and leaded to a decrease in $PM_{2.5}$ concentrations. In this particular case (during 00:00-07:00 14th), although the turbulent motions were weaker, the sub-mesoscale motions could form certain organized coherent structures. Consequently, we took this case for separate analysis, which implied that coherent sub-mesoscale structures may also contributes to the removal of $PM_{2.5}$.

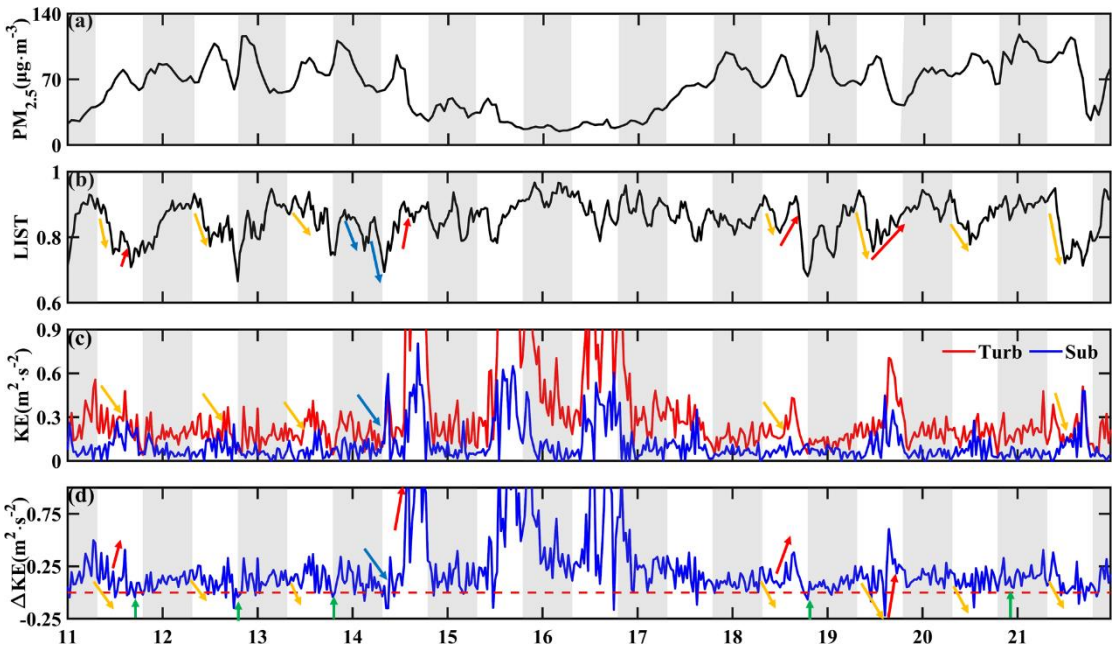

Figure 22. Time series of (a) PM2.5 concentration, (b) local intermittent strength of turbulence (LIST), (c) kinetic energy of turbulence (KE_{turb} solid red line) and kinetic energy of sub-mesoscale motion (KE_{sub} solid blue line), and (d) the kinetic energy difference ($\Delta KE = KE_{turb} - KE_{sub}$) from January 11 to 21, 2021. The gray shading represents night between 19:00 and 07:00 the following day. (From original manuscript Figure4)

Thanks again for the reviewer's comments. We need to emphasize it in the Page 14 Line 8 of original manuscript that the sub-mesoscale motions are not more efficient in mixing than turbulence. The details regarding the modifications are as follows:

The added manuscript: But this did not mean that the sub-mesoscale motions were more efficient in mixing than turbulence motions. It was just that we found a unique case in this study, which implied that the organized sub-mesoscale motions would also contribute to the removal of $PM_{2.5}$.

11. Page 14 Lines 5-11: If valid, why LIST increases on 21 Jan, but $PM_{2.5}$ decreases?

Response: Thank you for your helpful comments. As previously mentioned, the mixing efficiency of sub-mesoscale motions were lower in most instances. We explain the influence of the change of LIST over time on $PM_{2.5}$ concentration by introducing the definition and physical significance of LIST here.

With the help of SMT, Ren et al., (2019a, 2019b) proposed the local intermittent strength of turbulence (LIST) to quantitatively characterize turbulence intermittency

from the perspectives of kinetic energy of turbulence and sub-mesoscale motions. That is,

$$KE_{turb} = \frac{1}{2}\left(\overline{u'_{turb}}^{2} + \overline{v'_{turb}}^{2} + \overline{w'_{turb}}^{2}\right) \quad (1)$$

$$KE_{sub} = \frac{1}{2}\left(\overline{u'_{sub}}^{2} + \overline{v'_{sub}}^{2} + \overline{w'_{sub}}^{2}\right) \quad (2)$$

$$LIST = \frac{\sqrt{KE_{turb}}}{\sqrt{KE_{turb}+KE_{sub}}} \quad (3)$$

where the subscripts turb and sub represent the turbulent and sub-mesoscale parts, respectively. KE_{sub} is the kinetic energy of sub-mesoscale motions and KE_{turb} is the turbulent kinetic energy.

LIST characterizes the relative strength of turbulent and sub-mesoscale motions. Based on the previous understanding of turbulent intermittency, sub-mesoscale motions drive turbulent intermittency events, and changes in LIST can characterize turbulent intermittency events. When LIST decreases or maintains a small value, it means there is a strong influence of sub-mesoscale motions on weak turbulence, which may correspond to the period with weak fluctuation or even laminar flow in turbulent intermittency events (term as quiescent period). Alternatively, when LIST is maintained close to 1, this indicates that there is a very weak or even no influence of sub-mesoscale motions, which corresponds to pure turbulence. Between these two states, when LIST increases, this indicates a transition between weak turbulence and pure turbulence, which may correspond to transient turbulent bursts in turbulent intermittency events. The entire process of decreasing and increasing LIST to close to 1 corresponds to the occurrence of a complete turbulent intermittency event.

Our study cases indicated that when the LIST increased, that was, the role of turbulent motions gradually increased and the intermittency was weaker, this corresponded to a decrease in $PM_{2.5}$ concentration in most instances.

12. Page 15 Line 13: the figure can be shown in the supplementary.

Response: Thank you for your helpful comments. We have selected January 4th to10th as the representative of clean periods, which shows the same results as in the original manuscript. Additionally, we plan to intend to supplement Figure 23 in the

supplementary.

Page 15 Line 13 of original manuscript: For the sensible heat flux (Fig. 5e and 5f), during the clean periods (not shown in the figure), the ejections and sweeps (quadrants 1 and 3, black and blue solid lines) dominated throughout most of the day, presenting $\overline{w'\theta'} > 0$.

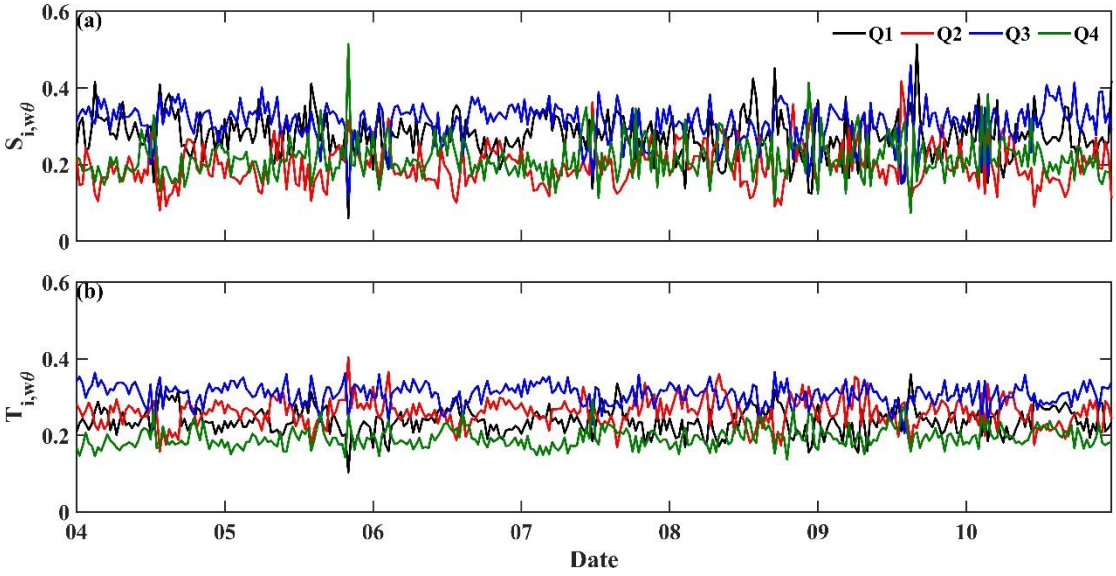

Figure 23. Time series of (a) flux contribution, and (b) time fraction of each quadrant for sensible heat flux from January 04 to 10, 2021(clean days). The solid black, red, blue, and green lines represent the results of the quadrants 1, 2, 3, and 4, respectively.

13. Page 16 Line 22: gust is due to the boundary-layer-scale turbulent eddies, not sub-mesoscale motions.

Response: We sincerely appreciate the reviewer's constructive comments regarding gust definitions. Given that you mentioned this issue, we deleted the description of gust-related definition from the original manuscript, but retained the possibility that the sub-mesoscale motions have some coherence.

The definition of gust may differ across various studies. Some research about the atmospheric boundary layer and atmospheric turbulence argued that strong winds are often accompanied by gusts with periods of 3 to 6 min, which are mixtures of low-frequency infrasonic waves and gravity waves, displaying a distinct coherent structure (Cheng et al., 2007; Zeng et al., 2010; Li et al., 2022). And gravity waves and low frequency infrasound are sub-mesoscale motions in the Mahrt's definition that we

followed. Zeng et al. (2010) further pointed out a correlation coefficient to quantify gust's coherence. Similarly, we also calculated the coherence of sub-mesoscale motions. We referred to this concept to illustrate that sub-mesoscale motions may also form a certain organizational structure.

Finally, thanks again for your helpful comments. We have deleted the description of gust-related definition from the original manuscript, but retained the possibility that the sub-mesoscale motions exhibit some coherence to study the effect of the organized sub-mesoscale motions on the matter transport in few hours.

14. The results are not well organized.

Response: We sincerely appreciate the reviewer's valuable comments. We realized that we did not clearly describe that: (1) the definition, the physical mechanism and the quantitative characterization of turbulence intermittency, (2) the definition and type of sub-mesoscale motions, and (3) the division basis between sub-mesoscale motions and turbulent motions in the original manuscript. Accordingly, we will implement significant improvements in both the introduction and methods sections, and supplement more detailed descriptions of time points in the sections of analysis and reorganized the results. These improvements enhance manuscript clarity and enable readers to directly find each conclusion to its supporting evidence.

15. Page 18 Lines 15-19: The plateau in the pre-multiplied u spectra may be due to attached eddies.

Response: Thank you for your constructive comments to our study. We would like to further elucidate the sub-mesoscale motions and turbulent motions on both sides of the spectrum gap, utilizing classical energy spectrum theory alongside the definition of the spectrum gap in atmospheric turbulence.

In the traditional turbulence theory, Van der Hoven (1957) presented an analysis on the large spectrum of horizontal wind speeds, which showed a notable spectral gap of approximately 1 cycle h^{-1} between the macroscale (synoptic) and microscale (turbulent) parts of the spectrum (see Figure 24). Many other studies have generally

proven the existence of the spectral gap (Panofsky, 1969; Fiedler and Panofsky, 1970; Smedman-Högström and Högström, 1975). There exists a gap in the energy spectral, and the large-scale motion associated with the lower frequency components tends to increase as frequency decreases. In this case, only the higher frequency part of the energy spectrum conforms to the classical turbulent energy spectrum model, that is, the energy-containing range, the inertial subrange, and the dissipation range.

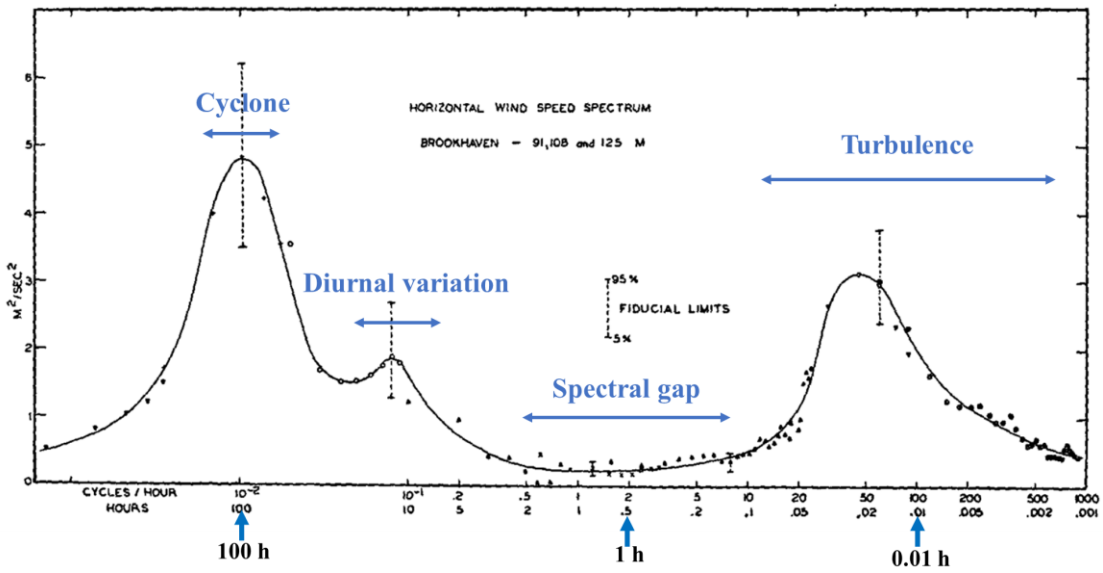

Figure 24. Horizontal wind-speed spectrum at Brookhaven National Laboratory at about 100-m height. (Cited from Van der Hoven., 2014, Figure 1)

Additionally, Vickers and Mahrt (2003) suggested that the gap scale is on the order of a few minutes or less in strong stratification or weak winds conditions. During the haze pollution periods, the wind speed was generally weak, and the time scale of the spectral gap was also smaller. Therefore, the low-frequency part of the gap was considered to be sub-mesoscale motions.

16. Fig. 6a2-d2: Pre-multiplied uw spectrum obeys a -4/3 scaling at small scales, which is not evident in Fig. 6a2-d2. Can the authors give a reason for this?

Response: Thank you for your valuable comments to our study. We would like to explain further by the following details why pre-multiplied uw spectra don't obey well the -4/3 scaling at small scales.

Firstly, the ordinate of Figure 6a2-d2 of original manuscript was not subjected to

logarithmic processing and normalization (see Figure 25a2-d2). Thus, the power law relationship could not be discerned. We adopted this processing method to quantify the magnitude and direction momentum flux transport. This approach used the area sizes and their corresponding signs under the covariance spectrum to determine these parameters when either sub-mesoscale or turbulent motions dominated. Specifically, when the spectral area greater than 0, it indicates - $\overline{u'w'} > 0$, corresponding to downgradient transport of momentum fluxes.

Subsequently, we performed logarithmic processing and normalization, as illustrated in the Figure 26. The results reveal that the power law is satisfied at small scales, however, the -4/3 scaling is not satisfied. The classical atmospheric boundary layer theories primarily focus on regions with uniform and flat underlying surfaces. In contrast, the complex underlying surfaces, especially urban aeras, often deviate from the classical theories (Roth and Oke, 1993; Roth, 2000). The presence of rough elements within the UCL causes the inertial subrange not follow well the traditional laws, and also changes in the high frequency small scale region. Which highlights the necessity of studying the characteristics of turbulence structures in the urban boundary layer, especially in the UCL.

Finally, we intend to replace Figure 6a2-d2 in original manuscript with Figure 26a2-d2 to show the power law relationship. Additionally, we would like to describe the magnitude and direction of the momentum fluxes transport when sub-mesoscale motions or turbulent motions dominate in the manuscript.

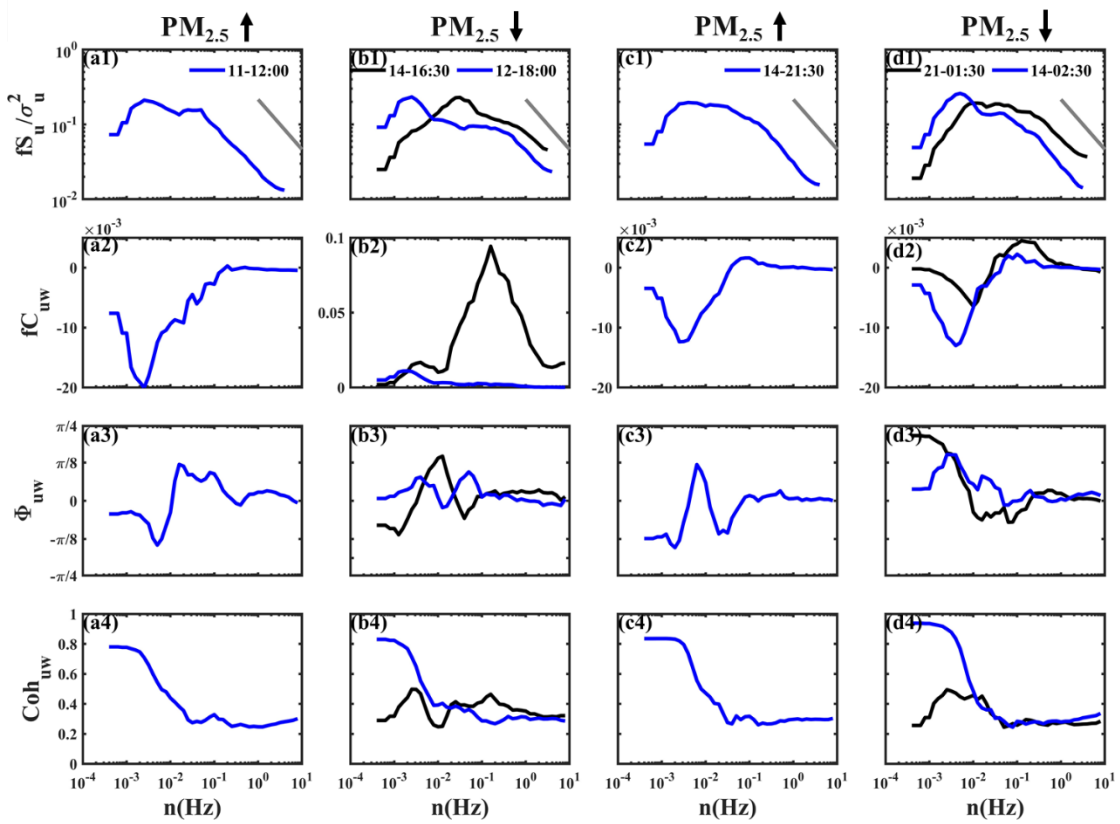

Figure 25. (a1–d1) Energy spectra of u, (a2–d2) covariance spectra of uw, (a3–d3) phase spectra of uw, and (a4–d4) coherence spectra of uw within the UCL of basin. Six time points were selected to represent the following: (a1-a4) 08:00–13:00 on the January 11, 2021, (b1-b4) 16:30 on the January 14, 2021 (solid black line) and 18:00 on the January 12, 2021 (solid blue line); (c1-c4) 21:30 on the on the January 14, 2021, (d1-d4) 01:30 on the on the January 21, 2021 (solid black line) and 02:30 on the January 14, 2021 (solid blue line). (From original manuscript Figure 6)

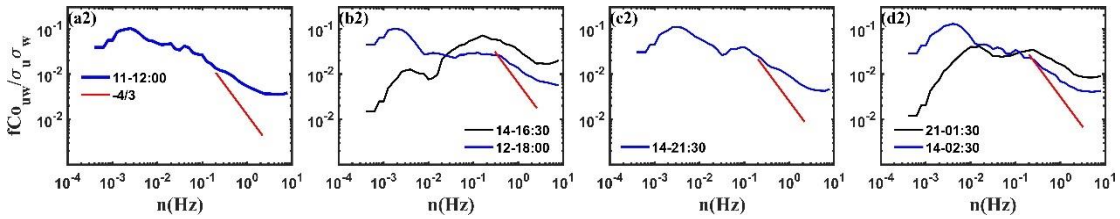

Figure 26. Normalized covariance spectrum of uw within the UCL

Minor comments:

1. Page 3 Line 4: UCL is urban canopy layer.

Response: We sincerely thank the reviewer for careful reading and careful checks. We have modified it.

2. Page 12 Line 5: ‘eddy eddies’ should be revised.

Response: We sincerely thank the reviewer for careful reading and careful checks. We have deleted ‘eddy’.

References

Acevedo, O. C., Costa, F. D., Oliveira, P. E. S., Puhales, F. S., Degrazia, G. A., and Roberti, D. R.: The influence of submeso processes on stable boundary layer similarity relationships, J. Atmos. Sci., 71, 207–225, https://doi.org/10.1175/JAS-D-13-0131.1, 2014.

Acevedo, O. C., and Fitzjarrald, D. R.: The influence of submeso processes on stable boundary layer similarity relationships, J. Atmos. Sci., 71, 207–225, https://doi.org/10.1175/JAS-D-13-0131.1, 2014.

Allouche, M., Bou-Zeid, E., Ansorge, C., Katul, G. G., Chamecki, M., Acevedo, O., Thanekar, S., and Fuentes, J. D.: The detection, genesis, and modeling of turbulence intermittency in the stable atmospheric surface layer, J. Atmos. Sci., 79, 1171–1190, https://doi.org/10.1175/JAS-D-21-0053.1, 2022.

Anfossi, D., Oetti, D., Degrazia, G., and Boulart, A.: An analysis of sonic anemometer observations in low wind speed conditions, Bound.-Layer Meteorol., 114, 179–203, https://doi.org/10.1007/s10546-004-1984-4, 2005.

Businger, J. A.: Turbulence transfer in the atmospheric surface layer, Workshop in Micro-meteorology, Am. Meteorol. Soc., 67–100, 1973.

Cava, D., Giostra, U., and Katul, G.: Characteristics of gravity waves over an Antarctic ice sheet during an austral summer, Atmosphere, 6, 1271–1289, https://doi.org/10.3390/atmos6091271, 2015.

Chang, H., Ren, Y., Zhang, H., Liang, J., Cao, X., Tian, P., Li, J., Bi, J., and Zhang, L.: The characteristics of turbulence intermittency and its impact on surface energy imbalance over Loess Plateau, Agric. Forest. Meteorol., 354, 110088, https://doi.org/10.1016/j.agrformet.2024.110088, 2024.

Chen, J., Zhao, C. S., Ma, N., Liu, P. F., Göbel, T., Hallbauer, E., Deng, Z. Z., Ran, L., Xu, W. Y., Liang, Z., Liu, H. J., Yan, P., Zhou, X. J., and Wiedensohler, A.: A

parameterization of low visibilities for hazy days in the North China Plain, Atmos. Chem. Phys., 12, 4935–4950, https://doi.org/10.5194/acp-12-4935-2012, 2012.

Cheng, X. L., Zeng, Q. C., Hu, F., and Peng, Z.: Gustiness and coherent structure of strong wind in the atmospheric boundary layer (in Chinese), Climatic Environ. Res., 12, 227–243, 2007.

Coulter, R. L., and Doran, J.: Spatial and temporal occurrences of intermittent turbulence during CASES-99, Bound.-Layer Meteorol., 105, 329–349, https://doi.org/10.1023/A:1019993703820, 2002.

Costa, F.D., Acevedo, O.C., Mombach, J.C.M., Degrazia, G.A.: A simplified model for intermittent turbulence in the nocturnal boundary layer. J. Atmos. Sci. 68 (8), 1714–1729, https://doi.org/10.1175/2011JAS3655.1, 2011.

Deb Burman, P. K. D., Prabha, T. V., Morrison, R., and Karipot, A.: A case study of turbulence in the nocturnal boundary layer during the Indian summer monsoon, Bound.-Layer Meteorol., 169, 115–138, https://doi.org/10.1007/s10546-018-0364-4, 2018.

Doran, J. C.: Characteristics of intermittent turbulent temperature fluxes in stable conditions, Bound.-Layer Meteorol., 112, 241–255, https://doi.org/10.1023/B:BOUN.0000027907.06649.d0, 2004.

Durden, D. J.: On the impact of wave-like disturbances on turbulent fluxes and turbulence statistics in nighttime conditions: a case study, Biogeosciences, 10, 8433–8443, https://doi.org/10.5194/bg-10-8433-2013, 2013.

Fernando, H. J. S.: Turbulent patches in a stratified shear flow, Phys. Fluids, 15, 3164–3169, https://doi.org/10.1063/1.1602076, 2003.

Fiedler, F., and Panofsky, H. A.: Atmospheric Scales and Spectral Gaps, B. Am. Meteorol. Soc., 51, 1114–1120, https://doi.org/10.1175/1520-0477(1970)051<1114:ASASG>2.0.CO;2, 1970.

Hiscox, A., Bhimireddy, S., Wang, J. M., Kristovich, D. A. R., Sun, J. L., Patton, E. G., Oncley, S. P., and Brown, W. O. J.: Exploring Influences of Shallow Topography in Stable Boundary Layers: the SAVANT Field Campaign, Bull. Am. Meteor. Soc., 104, 520–541, https://doi.org/10.1175/BAMS-D-21-0332.1, 2023.

Huang, Y. X., Schmitt, F. G., Lu, Z. M., and Liu, Y. L.: An amplitude-frequency study of turbulent scaling intermittency using empirical mode decomposition and Hilbert spectral analysis, Europhys. Lett., 84, 40010, https://doi.org/10.1209/0295-5075/84/40010, 2008.

Jia, W. X., Zhang, X. Y., Zhang, H. S., and Ren, Y.: Turbulent transport dissimilarities of particles, momentum, and heat, Environ. Res., 211, 113111, https://doi.org/10.1016/j.envres.2022.113111, 2022.

Ju, T. T., Wu, B. G., Zhang, H. S., Wang, Z. Y., and Liu, J. L.: Impacts of boundary-layer structure and turbulence on the variations of PM2.5 during Fog-Haze episodes, Bound.-Layer Meteorol., 183, 469–493, https://doi.org/10.1007/s10546-022-00691-z, 2022.

Kaimal, J. C., Wyngaard, J. C., Izumi, Y., and Coté, O. R.: Spectral characteristics of surface-layer turbulence, Quart. J. Roy. Meteor. Soc., 98, 563–589, https://doi.org/10.1002/qj.49709841707, 1972.

Katul, G. G., Albertson, J., and Parlange, M.: Conditional sampling, bursting, and the intermittent structure of sensible heat flux, J. Geophys. Res. Atmos., 99, 22869–22876, https://doi.org/10.1029/94JD01679, 1994.

Li, Q. L., Cheng, X. L., Ma, Y. B., Wu, L., and Zeng, Q. C.: Physical Model of Gusty Coherent Structure in Atmospheric Boundary Layer, J. Geophys. Res.-Atmos., 128, e2023JD038790, https://doi.org/10.1029/2023JD038790, 2023.

Li, X., Gao, C. Y., Gao, Z. Q., and Zhang, X. Y.: Atmospheric boundary layer turbulence structure for severe foggy haze episodes in north China in December, Environ. Pollut., 264, 114726, https://doi.org/10.1016/j.envpol.2020.114726, 2020.

Liu, C., Yang, Q., Shupe, M. D., Ren, Y., Peng, S., Han, B., and Chen, D.: Atmospheric turbulent intermittency over the Arctic Sea-ice surface during the MOSAiC expedition, J. Geophys. Res. Atmos., 128, e2022JD038790, https://doi.org/10.1029/2023JD038639, 2023.

Mahrt, L.: Nocturnal boundary-layer regimes, Bound.-Layer Meteorol., 88, 255–278, https://doi.org/10.1023/A:1001171313493, 1998.

Mahrt, L.: Stratified atmospheric boundary layers, Bound.-Layer Meteorol., 90, 375–

396, https://doi.org/10.1023/A:1001765727956, 1999.

Mahrt, L.: Weak-wind mesoscale meandering in the nocturnal boundary layer, Environ. Fluid Mech., 7, 331–347, https://doi.org/10.1007/s10652-007-9024-9, 2007.

Mahrt, L.: Characteristics of submeso winds in the stable boundary layer, Bound.-Layer Meteorol., 130, 1–14, https://doi.org/10.1007/s10546-008-9336-4, 2009.

Mahrt, L.: Variability and maintenance of turbulence in the very stable boundary layer, Bound.-Layer Meteorol., 135, 1–18, https://doi.org/10.1007/s10546-009-9463-6, 2010a.

Mahrt, L.: Computing turbulent fluxes near the surface: Needed improvements, Agric. For. Meteorol., 150, 501–509, https://doi.org/10.1016/j.agrformet.2010.01.015, 2010b.

Mahrt, L.: Stably stratified atmospheric boundary layers, Annu. Rev. Fluid Mech., 46, 23–45, https://doi.org/10.1146/annurev-fluid-010313-141354 2014.

Mahrt, L.: Microfronts in the nocturnal boundary layer, Q. J. Roy. Meteor. Soc., 145, 546–562, https://doi.org/10.1002/qj.3451, 2019.

Mahrt, L., and Bou-Zeid, E.: Non-stationary boundary layers, Bound.-Layer Meteorol., 177, 189–204, https://doi.org/10.1007/s10546-020-00533-w, 2020.

Mortarini, L., Cava, D., Giostra, U., Costa, F. D., Degrazia, G., Anfossi, D., and Acevedo, O.: Horizontal meandering as a distinctive feature of the stable boundary layer, J. Atmos. Sci., 76, 3029–3046, https://doi.org/10.1175/JAS-D-18-0280.1, 2019.

Muschinski, A., Frehlich, R.G., Balsley, B.B.: Smallscale and large-scale intermittency in the nocturnal boundary layer and the residual layer. J. Fluid Mech. 515, 319–351, https://doi.org/doi:10.1017/S0022112004000412, 2004

Pardyjak, E. R., Monti, P., and Fernando, H. J. S.: Flux Richardson number measurements in stable atmospheric shear flows, J. Fluid Mech., 459, 307–316, https://doi.org/10.1017/S0022112002008406, 2002.

Panofsky, H. A.: Spectra of atmospheric variables in the boundary layer, Radio Sci., 4, 1101–1109, https://doi.org/10.1029/RS004i012p01101, 1969.

Quan, J., Zhang, Q., He, H., Liu, J., Huang, M., and Jin, H.: Analysis of the formation

of fog and haze in North China Plain (NCP), Atmos. Chem. Phys., 11, 8205–8214, https://doi.org/10.5194/acp-11-8205-2011, 2011.

Ren, Y., Zhang, H. S., Wei, W., Wu, B. G., Cai, X. H., and Song, Y.: Effects of turbulence structure and urbanization on the heavy haze pollution process, Atmos. Chem. Phys., 19, 1041–1057, https://doi.org/10.5194/acp-19-1041-2019, 2019a.

Ren, Y., Zhang, H. S., Wei, W., Wu, B. G., and Liu, J. L.: Comparison of the turbulence structure during light and heavy haze pollution episodes, Atmos. Res., 230, 104645, https://doi.org/10.1016/j.atmosres.2019.104645, 2019b.

Ren, Y., Zhang, H. S., Wei, W., Cai, X., Song, Y., Kang, L., and Liu, J. L.: A study on atmospheric structure and intermittency during heavy haze pollution in the Beijing area, Sci. China Earth Sci., 62, 2058–2068, https://doi.org/10.1007/s11430-019-9451-0, 2019c.

Ren, Y., Zhang, H. S., Zhang, L., and Liang, J. N.: Quantitative description and characteristics of submeso motion and turbulence intermittency, Q. J. Roy. Meteor. Soc., 149, 1726–1744, https://doi.org/10.1002/qj.4479, 2023.

Ren, Y., Zhang, H. S., Zhang, X. Y., Cai, X. H., Song, Y., Liang, J. N., Zhang, L., Zhu, T., and Huang, J. P.: Research progress and current application of weak turbulence and turbulence intermittency in stable boundary layers, Earth-Sci. Rev., 262, 105062, https://doi.org/10.1016/j.earscirev.2025.105062, 2025.

Román-Cascón, C., Yagüe, C., Mahrt, L., Sastre, M., Steeneveld, G. J., Pardyjak, E., van de Boer, A., and Hartogensis, O.: Interactions among drainage flows, gravity waves and turbulence: a BLLAST case study, Atmos. Chem. Phys., 15, 9031–9047, https://doi.org/10.5194/acp-15-9031-2015, 2015.

Roth, M.: Review of atmospheric turbulence over cities, Q. J. Roy. Meteor. Soc., 126, 941–990, https://doi.org/10.1002/qj.49712656409, 2000.

Roth, M., and Oke, T. R.: Turbulent transfer relationships over an urban surface. I. Spectral characteristics, Q. J. Roy. Meteor. Soc., 119, 1071–1104, https://doi.org/10.1002/qj.49711951311, 1993.

Salmond, J. A.: Wavelet analysis of intermittent turbulence in a very stable nocturnal boundary layer: Implications for the vertical mixing of ozone, Bound.-Layer

Meteorol., 114, 463–488, https://doi.org/10.1007/s10546-004-2422-3, 2005.

Smedman-Högström, A. S., and Högström, U.: Spectral Gap in Surface-Layer Measurements, J. Atmos. Sci., 32, 340–350, https://doi.org/10.1175/1520-0469(1975)032<0340:SGISLM>2.0.CO;2, 1975.

Sun, J. L., Nappo, C. J., Mahrt, L., Belusic, D., Grisogono, B., Stauffer, D. R., Pulido, M., Staquet, C., Jiang, Q. F., Pouquet, A., Yagüe, C., Galperin, B., Smith, R. B., Finnigan, J. J., Mayor, S. D., Svensson, G., Grachev, A. A., and Neff, W. D.: Review of wave-turbulence interactions in the stable atmospheric boundary layer, Rev. Geophys., 53, 956–993, https://doi.org/10.1002/2015RG000487, 2015.

Van der Hoven, I.: Power Spectrum of Horizontal Wind Speed in the Frequency Range from 0.0007 to 900 Cycles Per Hour, J. Atmos. Sci., 14, 160–164, https://doi.org/10.1175/1520-0469(1957)014<0160:PSOHWS>2.0.CO;2, 1957.

Van der Linden, S. J. A., Van de Wiel, B. J. H., Petenko, I., Van Heerwaarden, C. C., Baas, P., and Jonker, H. J. J.: A Businger mechanism for intermittent bursting in the stable boundary layer, J. Atmos. Sci., 77, 1–48, https://doi.org/10.1175/JAS-D-19-0309.1, 2020.

Van de Wiel, B. J. H., Moene, A. F., Ronda, R. J., De Bruin, H. A. R., and Holtslag, A. A. M.: Intermittent turbulence and oscillations in the stable boundary layer over land. Part II: a system dynamics approach, J. Atmos. Sci., 59, 2567–2581, https://doi.org/10.1175/1520-0469(2002)059<2567:ITAOIT>2.0.CO;2, 2002.

Vercauteren, N., Boyko, V., Kaiser, A., Belušić, D., and Grisogono, B.: Statistical investigation of flow structures in different regimes of the stable boundary layer, Bound.-Layer Meteorol., 173, 143–164, https://doi.org/10.1007/s10546-019-00464-1, 2019.

Vickers, D., and Mahrt, L.: The cospectral gap and turbulent flux calculations, J. Atmos. Ocean. Technol., 20, 660–672, https://doi.org/10.1175/1520-0426(2003)20<660:TCGATF>2.0.CO;2, 2003.

Vickers, D., and Mahrt, L.: A solution for flux contamination by mesoscale motions with very weak turbulence, Bound.-Layer Meteorol., 118, 431–447, https://doi.org/10.1007/s10546-005-9003-y, 2006.

Vickers, D., and Mahrt, L.: Observations of the cross-wind velocity variance in the stable boundary layer, Environ. Fluid Mech., 7, 55–71, https://doi.org/10.1007/s10652-006-9010-7, 2007.

Wang, L. L., Fan, S. H., Hu, F., Miao, S. G., Yang, A. Q., Li, Y. B., Liu, J. K., Liu, C. W., Chen, S. S., Ho, H. C., Duan, Z. X., Gao, Z. Q., and Yang, Y. J.: Vertical gradient variations in radiation budget and heat fluxes in the urban boundary layer: a comparison study between polluted and clean air episodes in Beijing during winter, J. Geophys. Res.-Atmos., 125, e2020JD032478, https://doi.org/10.1029/2020JD032478, 2020.

Wei, W., Schmitt, F. G., Huang, X. Y., and Zhang, H. S.: The analyses of turbulence characteristics in the atmospheric surface layer using arbitrary-order Hilbert spectra, Bound.-Layer Meteorol., 159, 391–406, https://doi.org/10.1007/s10546-015-0122-9, 2016.

Wei, W., Zhang, H. S., Schmitt, F. G., Huang, Y. X., Cai, X. H., Song, Y., Huang, X., and Zhang, H.: Investigation of turbulence behaviour in the stable boundary layer using arbitrary-order Hilbert spectra, Bound.-Layer Meteorol., 163, 311–326, https://doi.org/10.1007/s10546-016-0227-9, 2017.

Wei, Z. R., Zhang, L., Ren, Y., Wei, W., Zhang, H. S., Cai, X. H., Song, Y., and Kang, L.: Characteristics of the turbulence intermittency and its influence on the turbulent transport in the semi-arid region of the Loess Plateau, Atmos. Res., 249, 105312, https://doi.org/10.1016/j.atmosres.2020.105312, 2021.

Zeng, Q. C., Cheng, X. L., Hu, F., and Peng, Z.: Gustiness and coherent structure of strong winds and their role in dust emission and entrainment, Adv. Atmos. Sci., 27, 1–13, https://doi.org/10.1007/s00376-009-8207-3, 2010.

Zhang, L., Zhang, H. S., Li, Q., Cai, X., and Song, Y.: Vertical dispersion mechanism of long-range transported dust in Beijing: effect of atmospheric turbulence, Atmos. Res., 269, 106033, https://doi.org/10.1016/j.atmosres.2022.106033, 2022.

Zhang, L., Zhang, H. S., Cai, X., Song, Y., and Zhang, X.: Characteristics of Turbulence Intermittency, Fine Structure, and Flux Correction in the Taklimakan Desert, J. Atmos. Sci., 81, 459–475, https://doi.org/10.1175/JAS-D-23-0107.1, 2024.

Zou, J., Liu, G., Sun, J. N., Zhang, H. S., and Yuan, R. M.: The momentum flux-gradient relations derived from field measurements in the urban roughness sublayer in three cities in China, J. Geophys. Res.-Atmos., 120, 10797–10809, https://doi.org/10.1002/2015JD023909, 2015.

Zhou, B., Chow, F.K.: Nested large-eddy simulations of the intermittently turbulent stable atmospheric boundary layer over real terrain. J. Atmos. Sci. 71 (3), 1021–1039, https://doi.org/10.1175/JAS-D-13-0168.1, 2014.